

PL-3-IRS66-0603

Technical Report # 198

FINAL REPORT  
FOR  
STUDY PROGRAM TO OBTAIN THE INFRARED  
INTERNAL REFLECTION SPECTRA OF POWDERED ROCKS

Prepared under  
NASA Contract #NASw-964 Mod. 1

Prepared for  
NATIONAL AERONAUTICS AND SPACE ADMINISTRATION  
Lunar and Planetary Programs  
Washington, D. C.

Prepared by  
PHILIPS LABORATORIES  
A Division of North American Philips Company, Inc.  
Briarcliff Manor, New York

June 1966

Principal Investigators:  
N. J. Harrick  
J. Bloxsom

A B S T R A C T

This study program is an extension of work previously conducted (NASA Contract NASW-964) to determine the feasibility of using Internal Reflection Spectroscopy for obtaining the infrared spectra of powdered rocks. In this earlier work, it was shown that infrared spectra characteristic of the material could be obtained for particles of any size (in this case, 0-43 $\mu$ ), and these spectra resembled those obtained via standard transmission techniques using very fine particles (less than 5 $\mu$ ). The samples were kaolinite-quartz mixtures, and the measurements were all made at an angle-of-incidence of 45°. The importance of these results - that spectra could be obtained for powders of any size and that no sample preparation was required - was such that further investigations were warranted. The present investigations (NASW-964 Mod. 1) verified the previous findings; pure quartz fractions were used, and the measurements were extended to other angles-of-incidence using polarized light. The spectra obtained, however, were dependent on polarization and particle size. This is attributed to the birefringent nature of quartz and to the large changes in the optical constants in the vicinity of absorption bands. As a demonstration of the practicality of Internal Reflection Spectroscopy, spectra were recorded of fourteen powdered mineral samples having particle sizes of 100 microns and less. These samples had been supplied to us by NASA. The spectra were similar to those recorded via transmission using powders of very small particle size (less than 5 $\mu$ ).

TABLE OF CONTENTS

Section	Page
ABSTRACT.....	ii
LIST OF ILLUSTRATIONS.....	iv
1. INTRODUCTION.....	1
2. OBJECTIVES.....	3
3. ACCOMPLISHMENTS.....	4
3.1 Summary.....	4
3.2 Particle Sizing and Purity Check of Quartz Powder.....	5
3.3 Modification For Varying Angle-of-Incidence..	11
3.4 90° Out-of-Phase Chopping.....	15
3.5 Spectra of Powdered Quartz Samples.....	17
3.6 Reflection Mechanism at Surface/Powder Interface.....	29
3.7 Methods for Quantitative Measurements.....	35
3.8 Comments on Measurements of Optical Constants via Internal Reflection Spectroscopy.....	36
3.9 Instrument Design Approach.....	39
3.10 Spectra of NASA-Supplied Powdered Rocks.....	40
4. CONCLUSIONS.....	59
5. RECOMMENDATIONS.....	61
6. REFERENCES.....	62

LIST OF ILLUSTRATIONS

	Page
Figure 1: Histogram of 0-3.5 $\mu$ Powdered Quartz Fraction....	7
Figure 2: Histogram of 10-20 $\mu$ Powdered Quartz Fraction....	8
Figure 3: Histogram of 20-30 $\mu$ Powdered Quartz Fraction....	9
Figure 4: Standard Transmission Spectra of 300 mg KBr Pellets Containing 0.17% Powdered Quartz Fractions.....	10
Figure 5: Functional Diagram of 90° Out-of-Phase Internal Reflection Spectrophotometer.....	12
Figure 6: Internal Reflection Spectra of Powdered Quartz Fractions Using $\theta = 60^\circ$ , Ge Plate, and <u>Perpendicular</u> Polarization.....	20
Figure 7: Internal Reflection Spectra of Powdered Quartz Fractions Using $\theta = 60^\circ$ , Ge Plate and <u>Parallel</u> Polarization.....	21
Figure 8: Internal Reflection Spectra of Powdered Quartz Fractions Using $\theta = 45^\circ$ , Ge Plate and <u>Perpendicular</u> Polarization.....	22
Figure 9: Internal Reflection Spectra of Powdered Quartz Fractions Using $\theta = 45^\circ$ , Ge Plate and <u>Parallel</u> Polarization.....	23
Figure 10: Internal Reflection Spectra of Powdered Quartz Fractions Using $\theta = 30^\circ$ , Ge Plate and <u>Perpendicular</u> Polarization.....	24
Figure 11: Internal Reflection Spectra of Powdered Quartz Fractions Using $\theta = 30^\circ$ , Ge Plate and <u>Parallel</u> Polarization.....	25
Figure 12: Internal Reflection Spectra of 0-3.5 $\mu$ Powdered Quartz Fraction Using Various Angles-of-Incidence, Ge Hemicylinder, and Different Polarization.....	26
Figure 13: Internal Reflection Spectra of 0-3.5 $\mu$ Powdered Quartz Fraction Using Various Angles-of-Incidence, GaAs Hemicylinder and Different Polarizations....	27

	Page
Figure 14: Internal Reflection Spectra of 10-20 $\mu$ Powdered Quartz Fraction Using Various Angles-of-Incidence, Ge Hemicylinder and Different Polarizations.....	28
Figure 15: Internal Reflection Spectra of Solid Quartz Crystal (A-T Cut) Using $\theta = 45^\circ$ , KRS-5 Hemicylinder, Perpendicular and Parallel Polarization, and Two Orientations of the Optical Axis With Respect to the Incident Light.....	33
Figure 16: Internal Reflection Spectra of Solid Quartz Crystal (A-T Cut) Using $\theta = 35^\circ$ , KRS-5 Hemicylinder, Perpendicular and Parallel Polarization, and Three Orientations of the Optical Axis With Respect to the Incident Light.....	34
Figure 17: Internal Reflection Spectra of 7.9 $\mu$ Absorption Band of Silicone Lubricant vs. Angle-of-Incidence.....	38
Figure 18: Internal Reflection Spectrum of Powdered Orthoclase Using $\theta = 45^\circ$ and KRS-5 Plate.....	43
Figure 19: Transmission and Internal Reflection Spectra ( $\theta = 45^\circ$ , KRS-5 Plate) of Powdered Albite.....	44
Figure 20: Internal Reflection Spectrum of Powdered Andesite (AGV-1) Using $\theta = 45^\circ$ and KRS-5 Plate.	45
Figure 21: Internal Reflection Spectrum of Powdered Labradorite Using $\theta = 45^\circ$ and KRS-5 Plate.....	46
Figure 22: Transmission and Internal Reflection Spectra ( $\theta = 45^\circ$ , KRS-5 Plate) of Powdered Augite.....	47
Figure 23: Internal Reflection Spectrum of Powdered Hedenbergite Using $\theta = 45^\circ$ and KRS-5 Plate.....	48
Figure 24: Internal Reflection Spectrum of Powdered Bronzite Using $\theta = 45^\circ$ and KRS-5 Plate.....	49
Figure 25: Internal Reflection Spectrum of Powdered Olivine Using $\theta = 45^\circ$ and KRS-5 Plate.....	50
Figure 26: Internal Reflection Spectrum of Powdered Dunite (DTS-1) Using $\theta = 45^\circ$ and KRS-5 Plate.....	51
Figure 27: Internal Reflection Spectrum of Powdered Fayalite Using $\theta = 45^\circ$ and KRS-5 Plate.....	52

## PHILIPS LABORATORIES

	Page
Figure 28: Internal Reflection Spectrum of Powdered Peridotite (PCC-1) Using $\theta = 45^\circ$ and KRS-5 Plate.....	53
Figure 29: Internal Reflection Spectrum of Powdered Basalt (BCR-1) Using $\theta = 45^\circ$ and KRS-5 Plate.....	54
Figure 30: Internal Reflection Spectrum of Powdered Granodiorite (GSP-1) Using $\theta = 45^\circ$ and KRS-5 Plate...	55
Figure 31: Internal Reflection Spectrum of Powdered Westerly Granite (G 2) Using $\theta = 45^\circ$ and KRS-5 Plate.....	56
Figure 32: Internal Reflection Spectra of Powdered Fayalite Using $\theta = 45^\circ$ , KRS-5 Plate and Perpendicular and Parallel Polarization.....	57
Figure 33: Internal Reflection Spectra of Powdered Rocks Using $\theta = 45^\circ$ , Ge Plate and Parallel Polarization.....	58

## PHILIPS LABORATORIES

### 1. INTRODUCTION

This study program is an extension of the work previously conducted by Philips Laboratories under NASA contract NASW-964 (Refs. 1,2). The purpose of the initial study was to determine the feasibility of using the technique of Internal Reflection Spectroscopy to obtain the infrared absorption spectra of powdered rocks.

Many samples to be analyzed are normally found in powdered form; other samples are so highly absorbing that they cannot be prepared in films sufficiently thin for conventional infrared transmission spectroscopy. Internal Reflection Spectroscopy has played an important role for analysis of solid highly absorbing samples as well as for powdered samples.

For analysis of strongly absorbing solid samples via internal reflection, it is only necessary to prepare one surface; the optical spectrum of the material can then be recorded by simply placing the sample in contact with a suitable transparent material (internal reflection element) of high refractive index. The desired contrast of the spectrum can be adjusted by appropriately selecting the refractive index of the internal reflection element, and adjusting the angle-of-incidence and/or number of reflections employed.

In some work at Philips Laboratories, it was shown that powdered samples can also readily be analyzed via internal reflection techniques. These results were verified in a study contract (NASA contract # NASW-964) where it was shown that for particles both smaller and larger than the wavelength of the light used, no scattering losses were observed in the non-absorbing regions and identical spectra, except for contrast, were recorded. When KBr pellets and conventional transmission techniques were used, it was only possible to obtain useful spectra for the small-diameter particles.

The powdered samples employed in this first study contract were kaolinite-quartz mixtures. The most important result was a confirmation of the absence of scattering. Because of the implications of these observations, it appeared desirable to continue this study and make similar measurements over a wide range of angles-of-incidence, employing pure quartz powders. It was hoped that this data would give us insight into the interaction

## PHILIPS LABORATORIES

mechanisms and perhaps an understanding of the reasons for the absence of scattering. Finally, internal reflection spectroscopy was to be employed to record the spectra of 14 powdered minerals supplied by NASA.

The objectives for this study are outlined in the following section.



## PHILIPS LABORATORIES

### 2. OBJECTIVES

The objectives of the program were as follows:

- a) Procure pure quartz powder and elutriate to particle sizes 0-3.5, 5-10, 10-20, 20-30, 30-50, and 50-100 microns. Check purity by taking x-ray diffraction patterns and standard infrared spectra of KBr pellets.
- b) Modify laboratory infrared spectrometer to make measurements at various angles-of-incidence, e.g., 15° to 75°. Fabricate and install variable-angle "vertical" double-pass plates. Fabricate GaAs plates to extend working range of spectrometer.
- c) Improve electronics by using 90° out-of-phase chopping to eliminate need for using optical nulls.
- d) Using elutriated quartz powder samples, take measurements at various angles-of-incidence using light polarized perpendicularly and parallel to the plane of incidence.
- e) Analyze and attempt to use data to obtain theoretical understanding of the reflection mechanism of the surface in contact with the powder.
- f) Study problem of measuring optical constants of powdered samples via internal reflection spectroscopy.
- g) Study sample collection, removal, and cleaning methods at high temperatures and high ('sticking') vacuum.
- h) Study and recommend methods for quantitative measurements.
- i) Recommend instrument design approach, i.e. source, detector, optics.
- j) Assess potential of the method by applying it to fourteen (14) powdered rock samples prepared for analysis and provided by NASA.

## PHILIPS LABORATORIES

### 3. ACCOMPLISHMENTS

#### 3.1 Summary

- a) Pure quartz crystals were pulverized and elutriated into a number of fractions of different particle sizes.
- b) The purity of the quartz powders was checked and verified via x-ray diffraction and via standard infrared spectra of KBr pellets. Particle sizes 0-3.5, 10-20, 20-30 microns were obtained.
- c) The laboratory infrared spectrometer was modified to make measurements at various angles-of-incidence.
- d) 90° out-of-phase chopping was incorporated into the laboratory infrared spectrometer.
- e) Internal reflection spectra were obtained of the following elutriated quartz powder fractions: 0-3.5, 10-20, 20-30 microns. Fixed-angle double-pass horizontal germanium plates were used. Measurements were made of the light polarized perpendicularly and parallel to the plane of incidence at angles-of-incidence of 30°, 45°, 60°. Measurements of reflectance at various angles-of-incidence near the critical angle were made using a variable-angle germanium internal reflection element, in attempt to obtain some information regarding the measurement of the optical constants of quartz.
- f) The data was analyzed, and a number of experimental facts were established. A theoretical model was formulated in an attempt to obtain a theoretical understanding of the interaction of the evanescent wave with the particulate matter.
- g) Methods for quantitative measurements were considered.
- h) Instrument designs were considered.
- i) Finally, to assess the potential of the method, spectra were obtained of fourteen (14) powdered mineral and rock samples which had been prepared for analysis and provided by NASA

### 3.2 Particle Sizing and Purity Check of Quartz Powder

The purity of the quartz powder was checked and verified via x-ray diffraction and via standard infrared spectra with KBr pellets. Particle sizes 0-3.5, 10-20, and 20-30 microns were obtained.

Crystalline mineral quartz was powdered and sized to below 100 microns by grinding and screening. The grinding and screening operations were performed by Lucius Pitkin, Inc. of New York City. All the powder passed through a 150 mesh screen; a portion of this powder was then reground until it passed through a 325 mesh screen. A portion was selected which had passed through the 150 mesh screen but did not pass through the 325 mesh screen. This portion was designated -150, +325 mesh.

The powder that passed through the 325 mesh screen was later elutriated by an Infrasizer. Since an Infrasizer is an instrument used in ore-dressing, the grouping into particle-sizes was not sharply delineated. Therefore, the fractions of quartz powder were subjected to particle-size analysis by a Coulter-type instrument at Interlab, Inc. of Harmon-on-Hudson, New York.

Histogram tables were prepared by Interlab. Total number of counts per fraction was 130,000; the electrolyte used was 40 grams of  $\text{Na}_4\text{P}_2\text{O}_7$  per liter of water. From an analysis of the data, three of the seven quartz powder fractions from the Infrasizer were selected to represent the 0-3.5, 10-20, and 20-30 micron samples.

Figures 1,2,3 are histograms of  $\Delta N$  vs.  $D$ , where  $\Delta N$  is the number of particles between two consecutive sizes and  $D$  is the diameter in microns of equivalent spheres. A cursory examination of the particles with an optical microscope showed approximately 30:1 ratio in the axial lengths of the particles. However, the data in histograms is given in terms of diameters of equivalent spheres. Figures 1,2,3 are histograms for quartz powder fractions of 0-3.5, 10-20, 20-30 microns, respectively. Since this Coulter-type instrument did not detect particles less than 1.5 microns, particle size distribution in the 0-1.5 micron range is not shown in Figure 1.

It was observed from the infrared spectra of the -150, +325 mesh that the presence of small particles negates the use of this fraction for the 50-100 micron fraction. An examination of Figure 4 will illustrate the similarity of spectra of the -150, +325 mesh and the 0-3.5 micron fraction.

## PHILIPS LABORATORIES

The selected fractions of quartz powder was subjected to x-ray analysis and to standard infrared spectral analysis with KBr pellets. A report from the X-ray Powder Diffractometry Laboratory of Philips Laboratories in Briarcliff Manor, New York, indicates that all the diffraction lines of 5-139, 5-142, 5-143, 5-145, corresponding to fraction sizes 50-100, 20-30, 10-20, and below 3.5 microns, respectively, were identified on the basis of a single (quartz) phase. No other phases were observed although cursory microscopic examination showed the presence of a small amount of a black impurity.

Standard infrared spectra (Figure 4) of quartz powders in KBr pellet form were obtained for the fractions 0-3.5, 10-20, and 20-30 microns. As mentioned previously, the -150, +325 mesh fraction was separated by screening, a process which has proven to be inadequate for the present investigation. KBr pellets (Harshaw Infrared Quality Potassium Bromide Powder) weighing 300 milligrams - each containing a 0.17% quartz fraction (0-3.5, 10-20, and 20-30 microns) - were examined, by transmission, in the 2.5 to 14 micron wavelength range. For the 0-3.5 micron fraction, the bands due to quartz (see Figure 4) are identified at 8.6, 9.2, 12.5 and 12.75 microns. Figure 4 shows that useful transmission spectra are not obtained from the larger fractions. Finally, it can be seen that the spectrum of the -150, +325 mesh fraction resembles the spectrum of the 0-3.5 micron fraction.

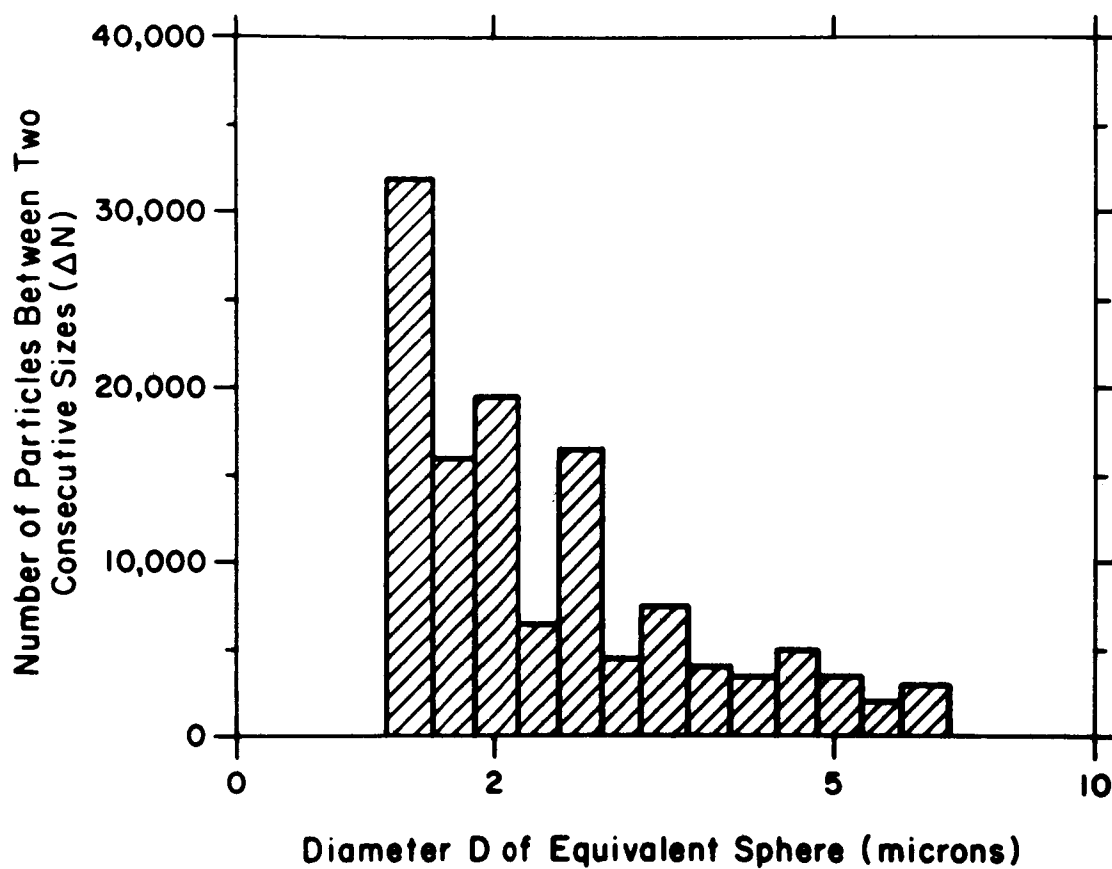


Figure 1: Histogram of 0-3.5 $\mu$  Powdered Quartz Fraction.

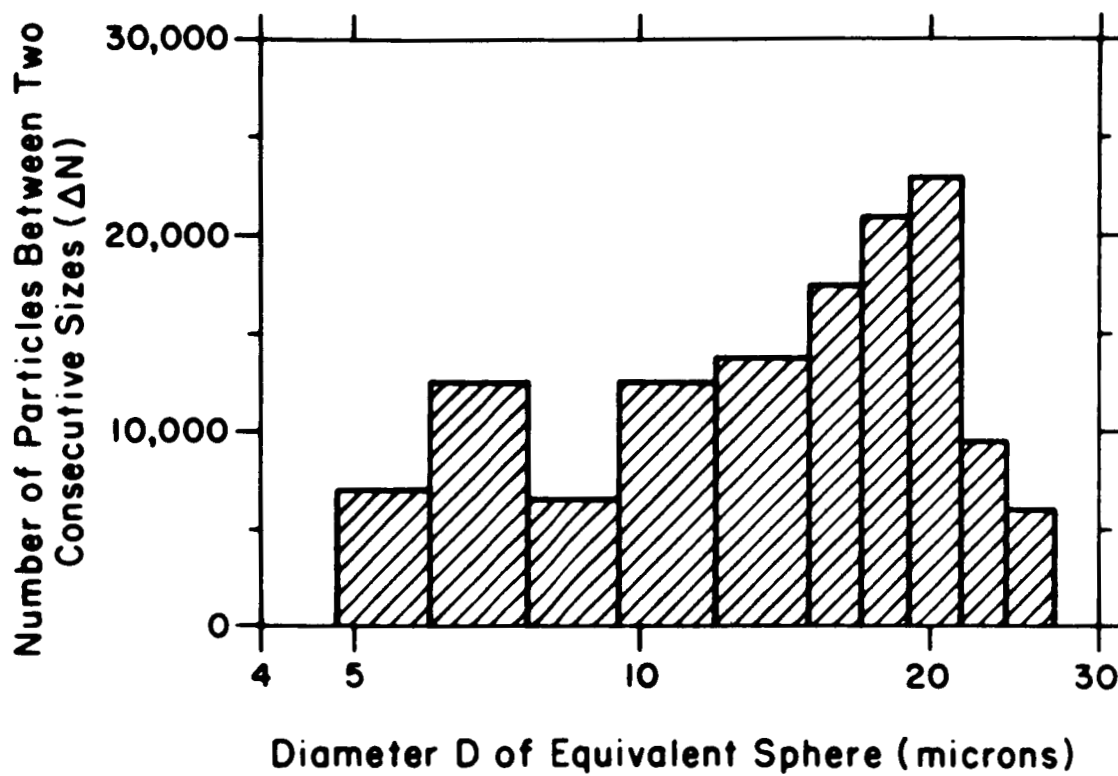


Figure 2: Histogram of 10-20  $\mu$  Powdered Quartz Fraction.

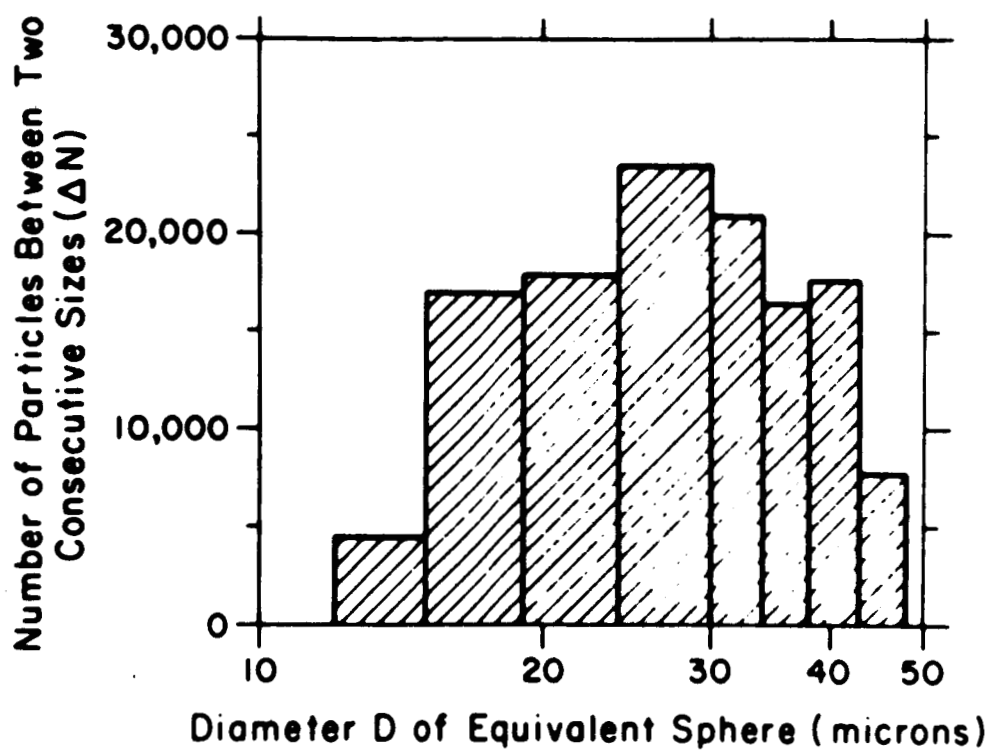


Figure 3: Histogram of 20-30  $\mu$  Powdered Quartz Fraction.

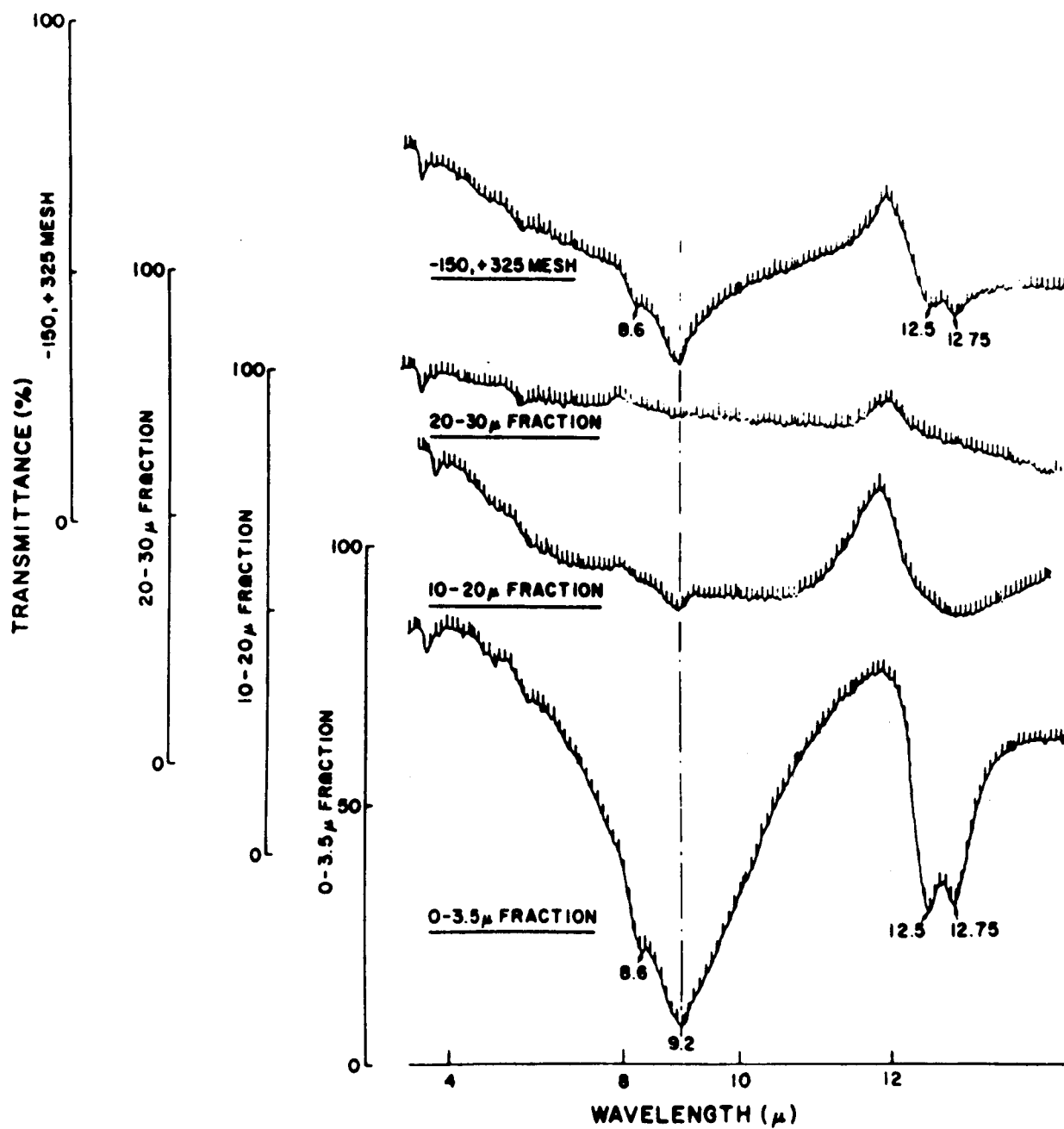


Figure 4: Standard Transmission Spectra of 300 mg KBr Pellets Containing 0.17% Powdered Quartz Fractions



### 3.3 Modification For Varying Angle-of-Incidence

#### 3.3.1 Spectrometer Modification

The laboratory infrared spectrometer was modified in order to facilitate measurements at various angles-of-incidence. The variable-angle attachment enables one to vary the angle-of-incidence on the internal reflection element; it also provides a direct reading of the angle selected. An important requirement for this device is that the exit rays from it must intersect the fixed mirrors of the spectrometer system such that there is no displacement of the rays with changes in angle-of-incidence. Without this requirement, it would be necessary to realign the spectrometer mirror system each time the angle-of-incidence is changed.

The modification to the spectrometer consisted of the incorporation of a device (Ref. 3) comprising a prism, internal reflection element, and a mirror for reflecting the light onto the prism. The device employs the principles of a right-angle mirror system. These principles are (1) the directions of the central entrance rays and the central exit rays are parallel, and (2) a rotation about the point of intersection of the two right-angle mirrors does not alter the distance between the entrance and exit rays. It should be noted (see Figure 5) that the internal reflection element is mounted on a surface which is perpendicular to the mirror which reflects the exit beam from the internal reflection element onto the prism.

The principles mentioned above will be considered via an analysis of the central rays of the variable angle attachment (see Figure 5). As far as the central rays are concerned, the back surface of the hemicylinder of the internal reflection element, and the surface to which it is mounted, can be considered as a plane mirror. The central rays of the incident light on the prism are parallel to the base of the right-angle prism. The surface on which the internal reflection element is mounted and the mirror used to reflect the exit light from the internal reflection element constitute a right-angle mirror system. The vertex of the right-angle prism and the vertex of the right-angle mirror system are located on a line perpendicular to the base of the right-angle prism.

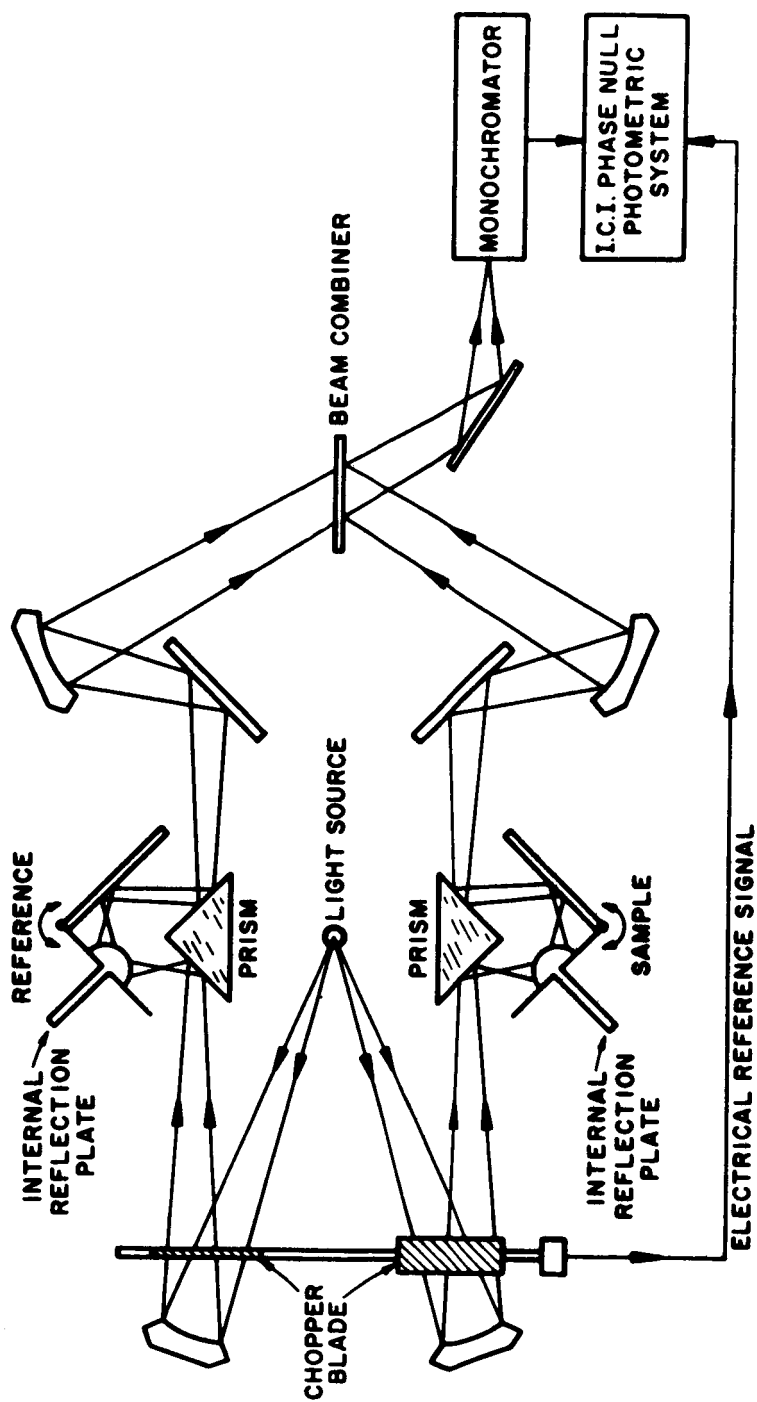


Figure 5: Functional Diagram of 90° Out-of-Phase Internal Reflection Spectrophotometer

### 3.3.2 Analysis of Variable-Angle Attachment

Principle # 1. One important property of the device is that the direction of the reflected central ray from the right-angle prism to the surface H must be parallel to the reflected central ray from the reflecting mirror whose purpose is to reflect the exit light from the internal reflection element onto the prism, independent of rotations about the vertex of the right-angle mirror system. Rotation about the point of intersection of the "two" right-angle mirrors causes the reflected central rays from the prism to intersect "mirror" H at different distances from the point of intersection of the "two" right-angle mirrors.

Let A be the point of intersection of the central rays on the mirror surface (H), let B be the point of intersection of the "two mirrors", and let C be the point of intersection of the exit central rays on the mirror surface used to reflect these rays onto the prism. A rotation of angle  $\alpha$  about point B makes angle  $CAB = \pi/2 - (\pi/4 - \alpha) = \pi/4 + \alpha$ . As angle  $ACB = \pi/4 - \alpha$ , and since angle  $ACB$  plus angle  $CAB = \pi/2$  and angle  $CBA$  is a right-angle for a right-angle mirror system, the incident angle to the normal at C is  $\pi/2 - (\pi/4 - \alpha) = \pi/4 + \alpha$ . The reflection angle to this normal is  $\pi/4 + \alpha$ . Therefore, the sum of the interior angles between the entrance central rays at point A and the exit central rays from point C is  $\pi/4 - \alpha + \pi/4 + \alpha + \pi/4 + \alpha = \pi$ .

However, the sum of interior angles between two parallel lines is  $\pi$ , and conversely. Therefore, the exit central rays from C are parallel to the incident central ray on A, independent of the rotation of the mirror about point B.

Principle # 2. The other important property of the device may be exhibited now that it has been established that the entrance central rays to the right-angle mirror system and the exit central rays from the right-angle mirror system are parallel. This property is that the distance ( $d_1$ ) between the entrance central rays to the right-angle mirror system and the line drawn through the vertex of the right-angle prism and point B is equal to the distance ( $d_2$ ) from the latter line to the exit central rays from the right-angle mirror system. Clearly, for  $45^\circ$  angle-of-incidence on the right-angle mirror system,  $d_1 = d_2$  by symmetry. For this condition, if  $\alpha$  is the angle of rotation about point B, let  $\alpha$  equal zero. Therefore,  $\alpha$  represents a rotation from this symmetrical condition. Using polar coordinates, let  $r_1$  be the

distance from point B to intersection (point A) of entrance central rays to the right-angle mirror system and  $r_2$  be the distance from point B to the intersection (point C) of exit central rays to the reflecting mirror to the prism.

$$d_1 = r_1 \sin (\pi/4 + \alpha)$$

$$d_2 = r_2 \sin (\pi/4 - \alpha)$$

$$\frac{d_1}{d_2} = \frac{r_1 \sin (\pi/4 + \alpha)}{r_2 \sin (\pi/4 - \alpha)}$$

Using the law of sines for this triangle ABC,

$$\frac{r_1}{r_2} = \frac{\sin (\pi/4 - \alpha)}{\sin (\pi/4 + \alpha)}$$

$$\frac{d_1}{d_2} = \frac{\sin (\pi/4 - \alpha)}{\sin (\pi/4 + \alpha)} \frac{\sin (\pi/4 + \alpha)}{\sin (\pi/4 - \alpha)}$$

$$= 1 \text{ for arbitrary values of } \alpha$$

Therefore,  $d_1 = d_2$  for all angles of rotation.

Since rotation of the variable-angle attachment displaces the variable-angle internal reflection element, two translations are required in order to correct for defocussing and for displacement of the incident light relative to the variable-angle internal reflection element. These translations are accomplished by mounting the entire variable-angle assembly on a two-stage micro-manipulator.

### 3.4 90° Out-of-Phase Chopping

#### 3.4.1 Principle of Operation

Ninety-degree out-of-phase chopping was incorporated into the laboratory infrared spectrometer. The system uses a Phase Null Photometric System designed by Instruments and Communications, Inc. of Wilton, Connecticut for Philips Laboratories.

The principle of operation of the spectrophotometer is briefly as follows: The vector addition of two sinusoidal waves of the same frequency (in this case, 17 cycles/sec.), but different in phase by 90°, results in a sinusoidal wave whose phase - relative to one of the components - varies as the arc-tangent of the ratio of the amplitudes of the original waves. In this system, two 90° out-of-phase optical signals (sample and reference) are generated via mechanical choppers. In addition, two electrical signals, 90° out-of-phase with each other and fixed in phase relative to the optical signal, are generated through a photocell phase-shifting network associated with the chopper. The two optical signals are summed in the monochromator detector; the two electrical signals (analogous to the sample and reference optical signals) are summed by electronic circuitry. Thus, two sinusoidal waves have been generated whose phase angles are a function of the ratio of their respective components.

The I.C.I. Phase Null Photometric System compares the phase of the optical resultant sinusoidal wave with the phase of the resultant electronically-generated wave, and adjustments are made on the phase of the electrically-generated sinusoidal wave to produce a null. The phase angles of the two signals are now identical, and the ratio of their components are therefore the same. Since the "reference" component of the electronically-generated signal is constant, a measurement of the "sample" component of the electronically-generated signal is proportional to the ratio of the electronically-generated signals and, thus, to the ratio of the components of the resultant optical signal.

The original design frequency was 12 cycles per second but electrical disturbances created by other 12 cycles per second systems required that the frequency be changed to 17 cycles per second. Also, coherent electromagnetic fields generated

by rotating magnetic fields required the use of a photo-optical phasing detector for establishing a common reference phase for the optically-generated signals and the electronically-generated signals.

### 3.4.2 Signal Processing

Any corresponding points, in time, on each of the two waves (optical, electrical) can be used for comparing the wave phases; in this particular case, the zero-crossing points (where the wave goes through zero) are adjusted to correspond in time. By so doing, their phases correspond, and, therefore, the ratio of their respective wave components are equal. The following paragraphs describe the signal processing involved.

The output of the thermocouple detector (Reeder RP-3W) from the monochromator is sent to the Phase Null Photometric System where the following operations are performed. The signal is first preamplified and then wave-shaped and amplified by a tuned amplifier. This signal, a 17 cycle/sec sinusoidal wave, is then shaped into a square wave by a "zero-crossing" circuit. This circuit is called "zero-crossing" because the steps of the square wave correspond to the zero points of the sinusoidal wave. It should be noted that the zero crossings shift with change in phase of the wave. These pulses are then sent to a comparison circuit where they are compared with corresponding pulses from the electronically-generated signal.

Pertaining to the electronically-generated wave, a photocell detector in conjunction with the mechanical chopper is used to produce an electrical reference signal. This signal is wave shaped and amplified by a tuned amplifier to produce a 17 cps sinusoidal wave. It is then passed through a phase shifting circuit to produce two signals differing in phase by  $90^\circ$ . These two signals are added vectorially by an adding circuit, passed through a "zero-crossing" circuit, a differentiating circuit, and finally to the comparison circuit.

The output of the comparison circuit is used by an electronic servo circuit for adjusting one of the two signal components of the electronically-generated wave. This adjustment equalizes the phases of the electronically-generated and optically-generated waves. Since the ratio of the components of each wave are now equal, measurement of the ratio of the wave components of the electronically-generated wave is equivalent to measuring the ratio of the optically-generated wave components. This measured ratio is then fed to an x-y pen recorder.

### 3.5 Spectra of Powdered Quartz Samples

Internal reflection spectra were obtained of the following elutriated quartz powder fractions: 0-3.5, 10-20, 20-30 microns. Fixed-angle double-pass horizontal germanium plates were used. Measurements were made of the light polarized perpendicularly and parallel to the plane-of-incidence, using angles-of-incidence of  $30^\circ$ ,  $45^\circ$ ,  $60^\circ$ . By perpendicular polarization we mean that the electric vector plane of vibration is perpendicular to the plane-of-incidence; by parallel polarization we mean that the electric vector plane of vibration is parallel to the plane-of-incidence. Using elutriated quartz powder samples, measurements of reflectance at various angles-of-incidence were also made near the critical angle, using germanium and gallium arsenide internal reflection elements (hemicylinders). These latter measurements yield dispersion-type spectra which are useful for determining optical constants.

There are general characteristics of the internal reflection spectra of the powdered quartz fractions that can be best seen by placing the spectra of the three fractions on the same graph. The ordinate scale of the spectra is in percent reflectance; the abscissa is given as wavelength in microns. The family of curves are displaced along the ordinate to facilitate comparison, and each curve retains its zero to one hundred percent ordinate scale. The angle-of-incidence and state of polarization are indicated on each graph. A comparison line at 9.2 microns is shown on each figure; this is the position of the absorption band of powdered quartz as established from Figure 4. The characteristics of the spectra are as follows:

- a) For perpendicular polarization, the reflectance minima are shifted to longer wavelengths relative to 9.2 microns and occur at approximately 9.6 microns.
- b) For parallel polarization, the reflectance minima are shifted to the shorter wavelengths relative to 9.2 microns and are dependent on particle-size.
- c) For parallel polarization, the location of the band at 8.6 microns is somewhat independent of particle-size.

Figures 6 through 11 are internal reflection spectra of the powdered quartz fractions using 60°, 45°, 30° angles-of-incidence, germanium double-pass plates, and perpendicular and parallel polarizations. The following table tabulates the reflectance minima near the 9 micron region.

It should be noted that the locations of the bands are substantially independent of the angle-of-incidence  $\theta$  for the 0-3.5  $\mu$  fraction. However, for  $\theta = 30^\circ$ , there is a shift towards the longer wavelengths for the larger fractions. A shift towards longer wavelengths with decrease of  $\theta$  is characteristic of internal reflection measurements on bulk materials.

Table I: Locations of Reflectance Minima Near 9 $\mu$  Region

$\theta$	Quartz Fraction 0-3.5 $\mu$		Quartz Fraction 10-20 $\mu$		Quartz Fraction 20-30 $\mu$	
	Polarization		Polarization		Polarization	
	Perpend.	Parallel	Perpend.	Parallel	Perpend.	Parallel
60°	9.4 $\mu$	9.2 $\mu$	9.45 $\mu$	8.7 $\mu$	9.5 $\mu$	8.5 $\mu$
45°	9.5 $\mu$	9.2 $\mu$	9.55 $\mu$	8.7 $\mu$	9.6 $\mu$	8.5 $\mu$
30°	9.5 $\mu$	9.2 $\mu$	9.7 $\mu$	8.8 $\mu$	9.7 $\mu$	8.7 $\mu$

Figure 12 presents the internal reflection spectra of the 0-3.5 $\mu$  powdered quartz fraction using a variable-angle germanium hemicylinder and various states of polarization. The curves illustrate the displacement of the minima to longer wavelengths in the region of 9.2 microns, for perpendicular polarization and  $\theta = 45^\circ$ . For angles-of-incidence below the critical angle (20°, 18°, 16°, 15°), there is a small shift in the minima toward the longer wavelengths.

Figure 13 shows the internal reflection spectra of the 0-3.5 $\mu$  powdered quartz fraction using a variable-angle gallium arsenide hemicylinder and various states of polarization. The curves illustrate the expected displacement of the 9.2 micron minima to longer wavelengths for perpendicular polarization and a displacement of these minima to shorter wavelengths for parallel polarization. The other curves illustrate the expected displacement



## PHILIPS LABORATORIES

of the minima toward longer wavelengths for angles-of-incidence less than the critical angle with the gallium arsenide/quartz system. In addition, there is a reduction in the contrast of the spectra near 9 microns for angles-of-incidence below the critical angle.

Figure 14 presents the internal reflection spectra of the 10-20 $\mu$  powdered quartz fraction using a variable-angle germanium hemicylinder and different states of polarization. The reduction in contrast of the spectra for angles-of-incidence below the critical angle and near the 9 micron region can be seen in this larger particle-size fraction.

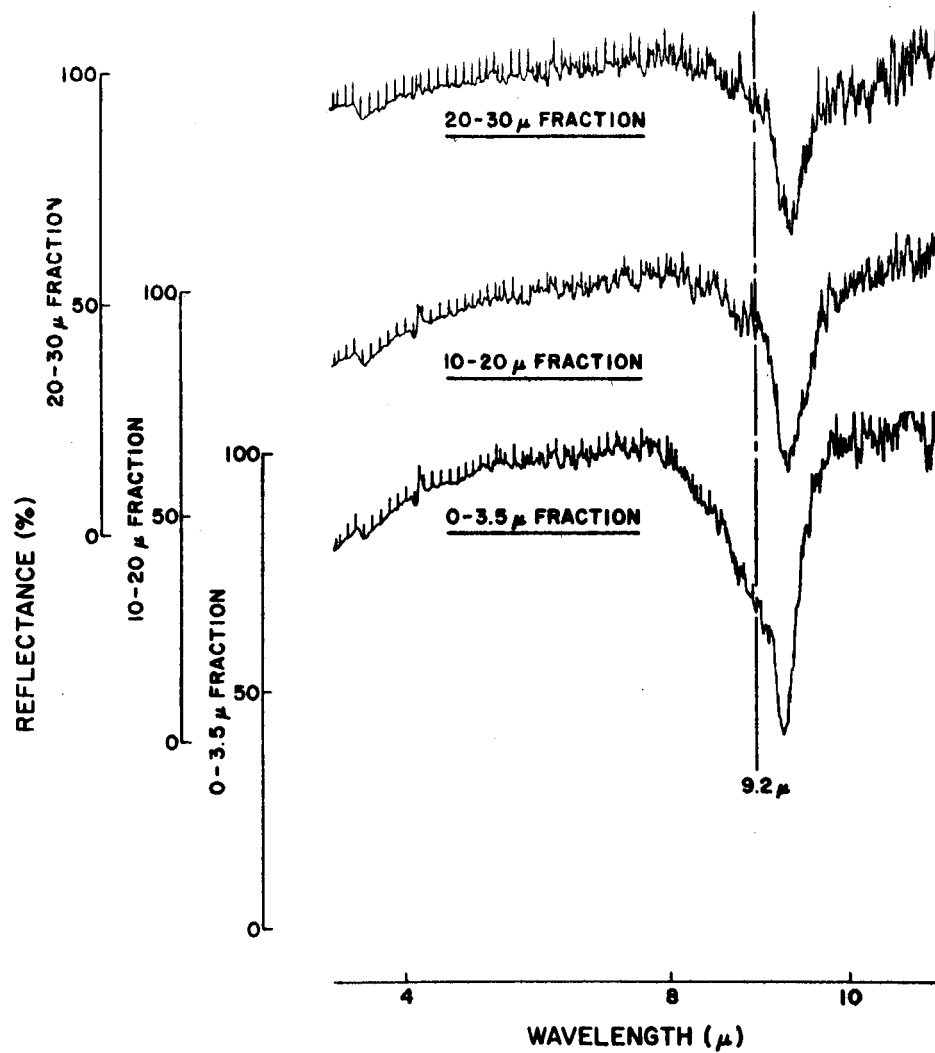


Figure 6: Internal Reflection Spectra of Powdered Quartz Fractions  
Using  $\theta = 60^\circ$ , Ge Plate, and Perpendicular Polarization.

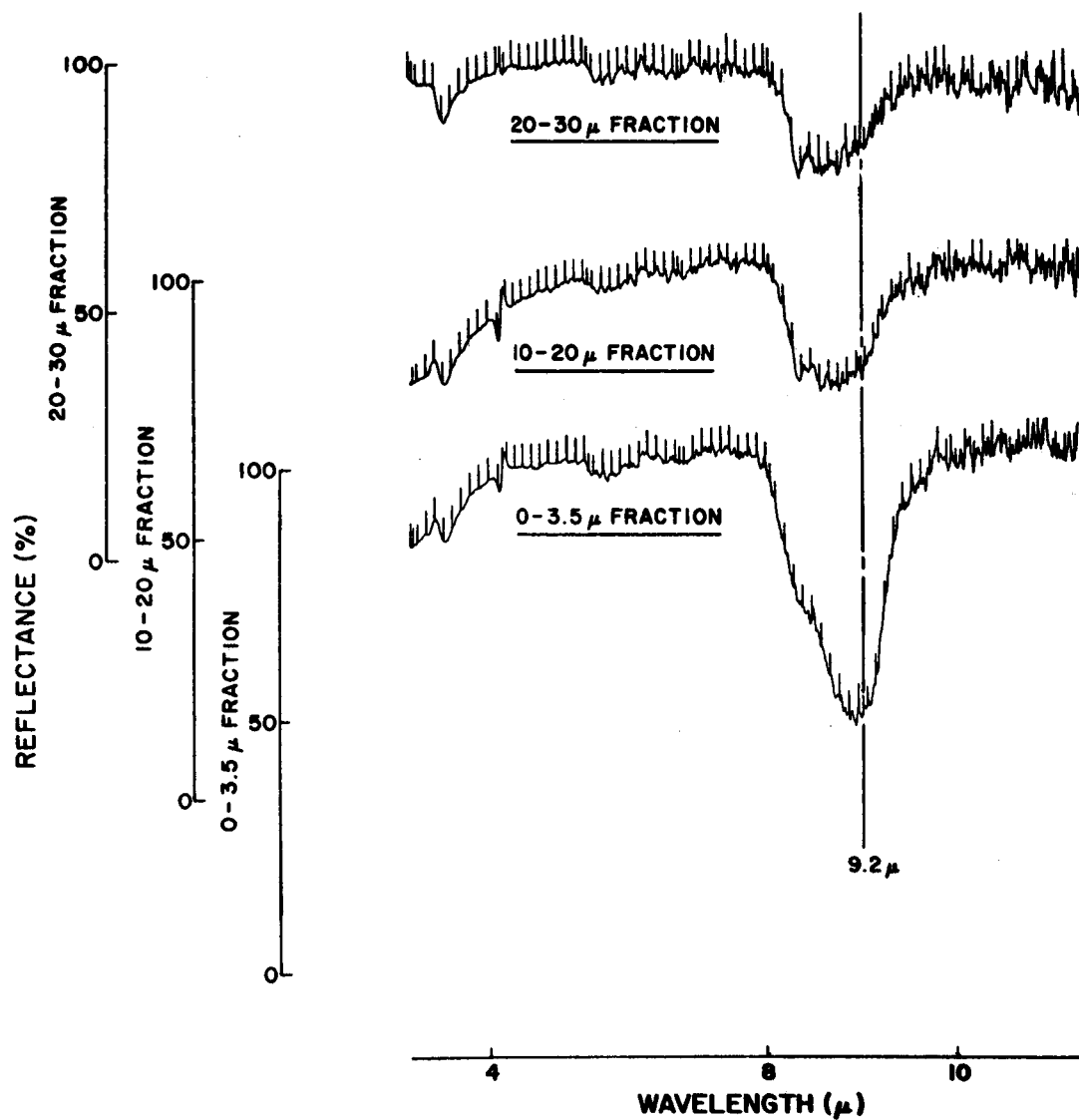


Figure 7: Internal Reflection Spectra of Powdered Quartz Fractions  
Using  $\theta = 60^\circ$ , Ge Plate, and Parallel Polarization.

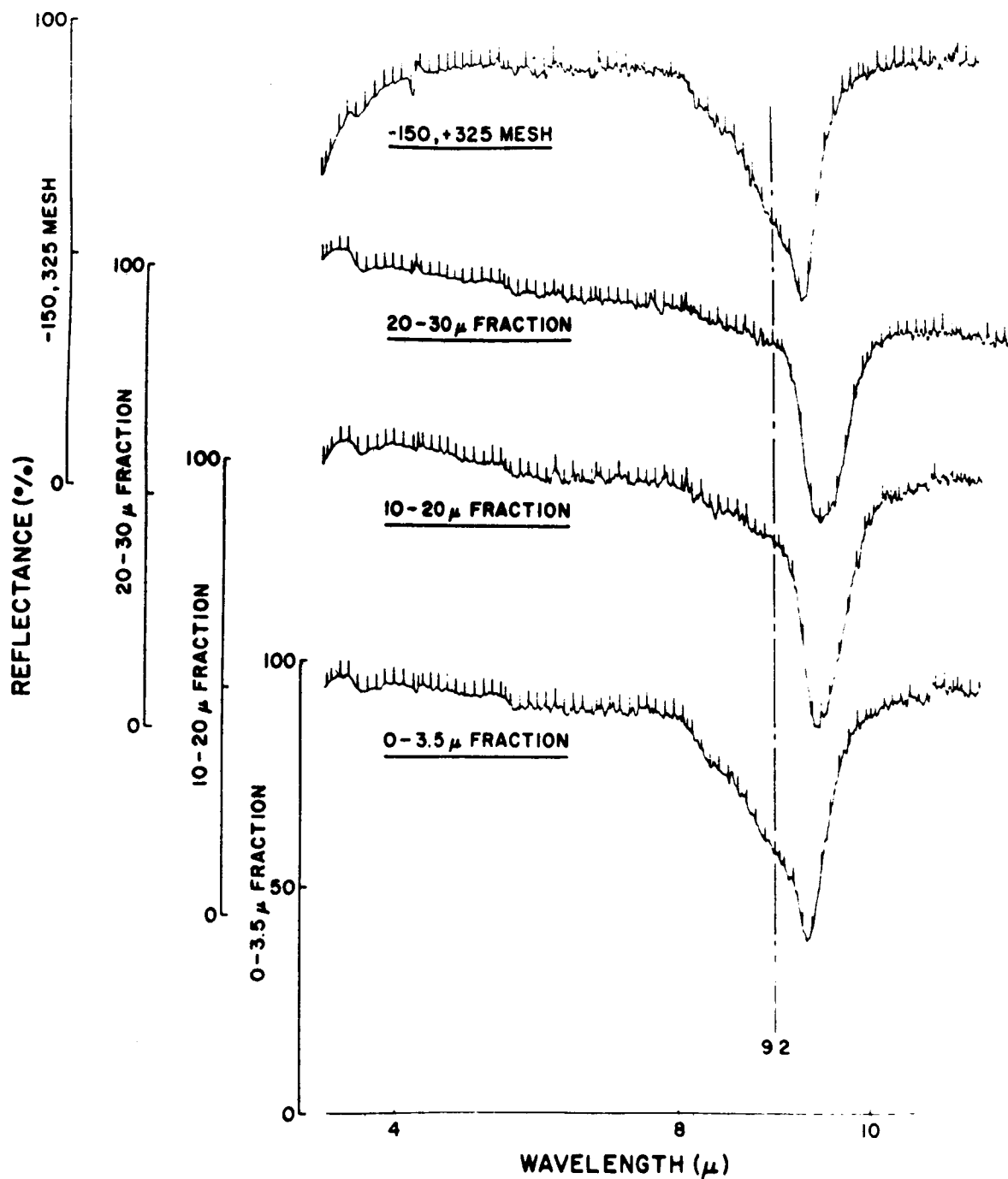


Figure 8: Internal Reflection Spectra of Powdered Quartz Fractions Using  $\theta = 45^\circ$ ,  
Ge Plate and Perpendicular Polarization

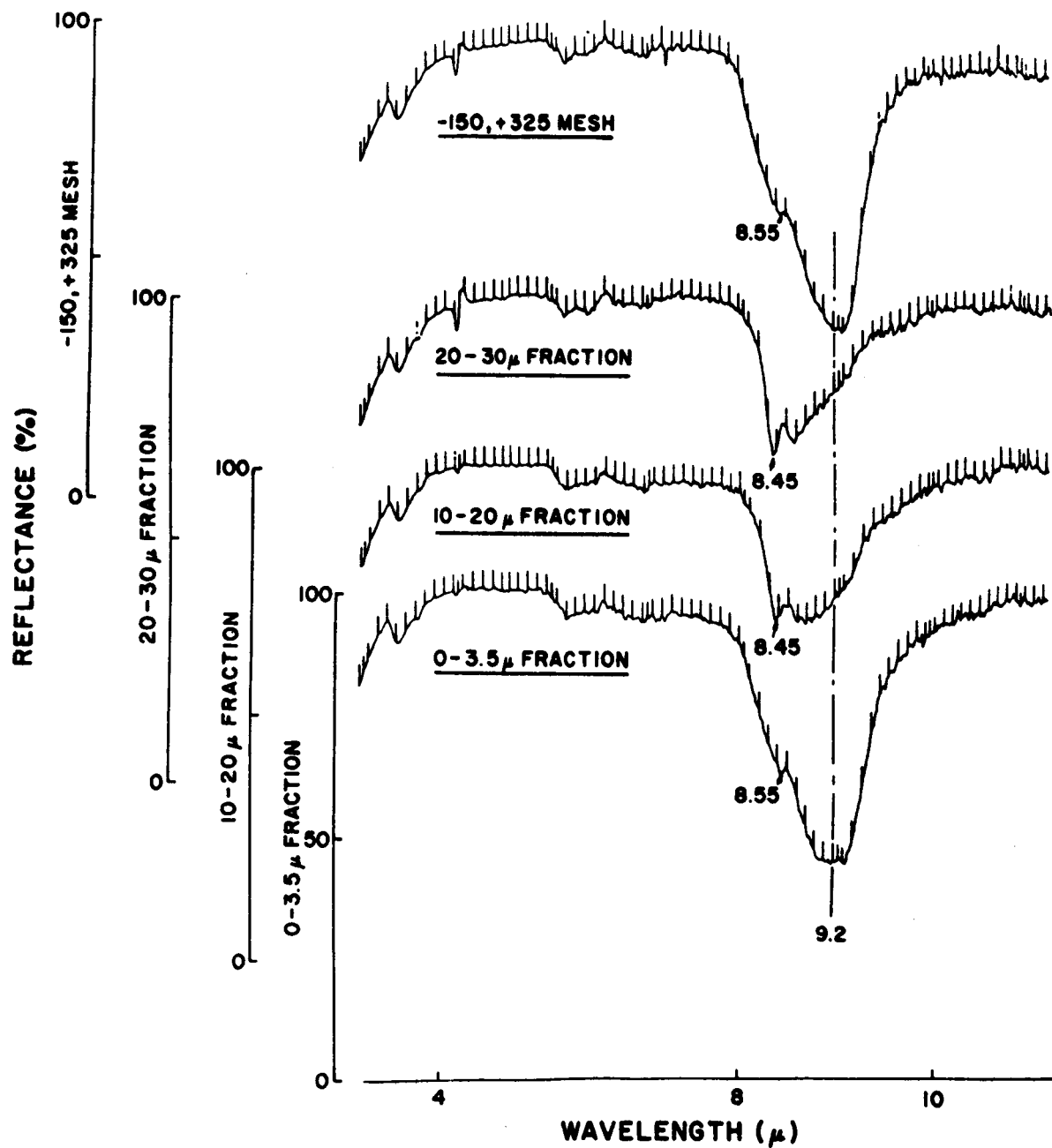


Figure 9: Internal Reflection Spectra of Powdered Quartz Fractions Using  $\theta = 45^\circ$ , Ge Plate and Parallel Polarization

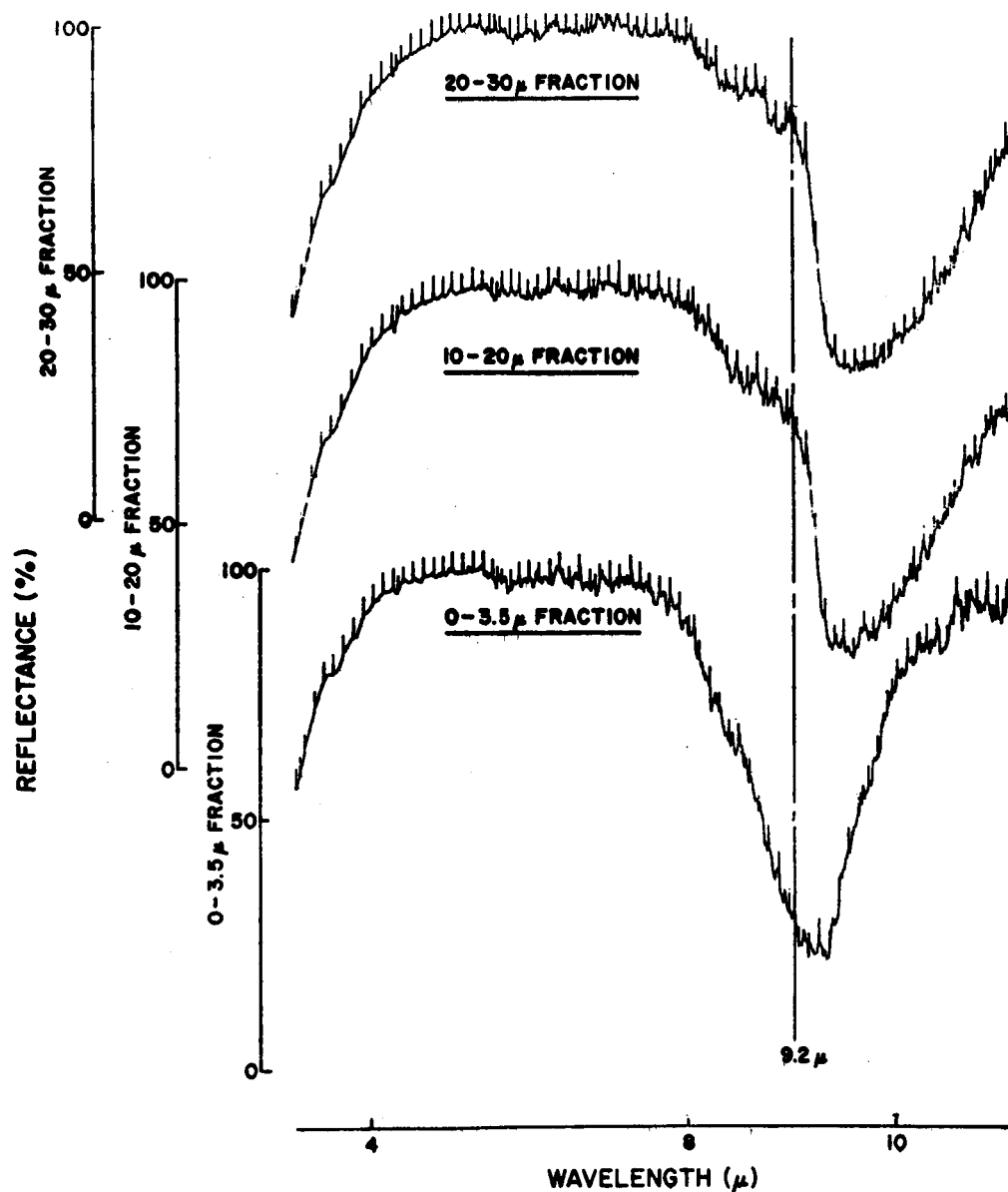


Figure 10: Internal Reflection Spectra of Powdered Quartz Fractions  
Using  $\theta = 30^\circ$ , Ge Plate, and Perpendicular Polarization.

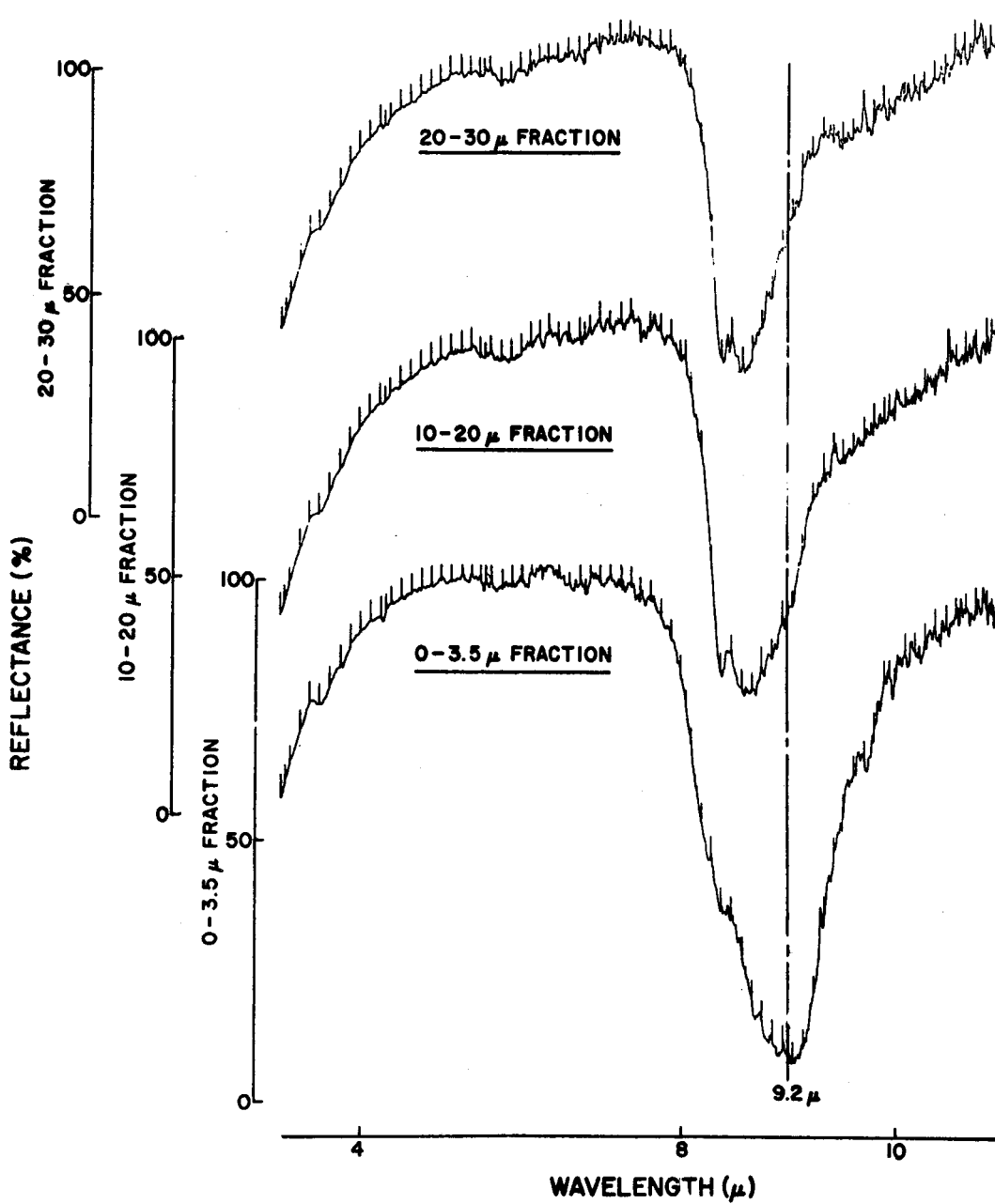


Figure II: Internal Reflection Spectra of Powdered Quartz Fractions Using  $\theta = 30^\circ$ , Ge Plate, and Parallel Polarization.

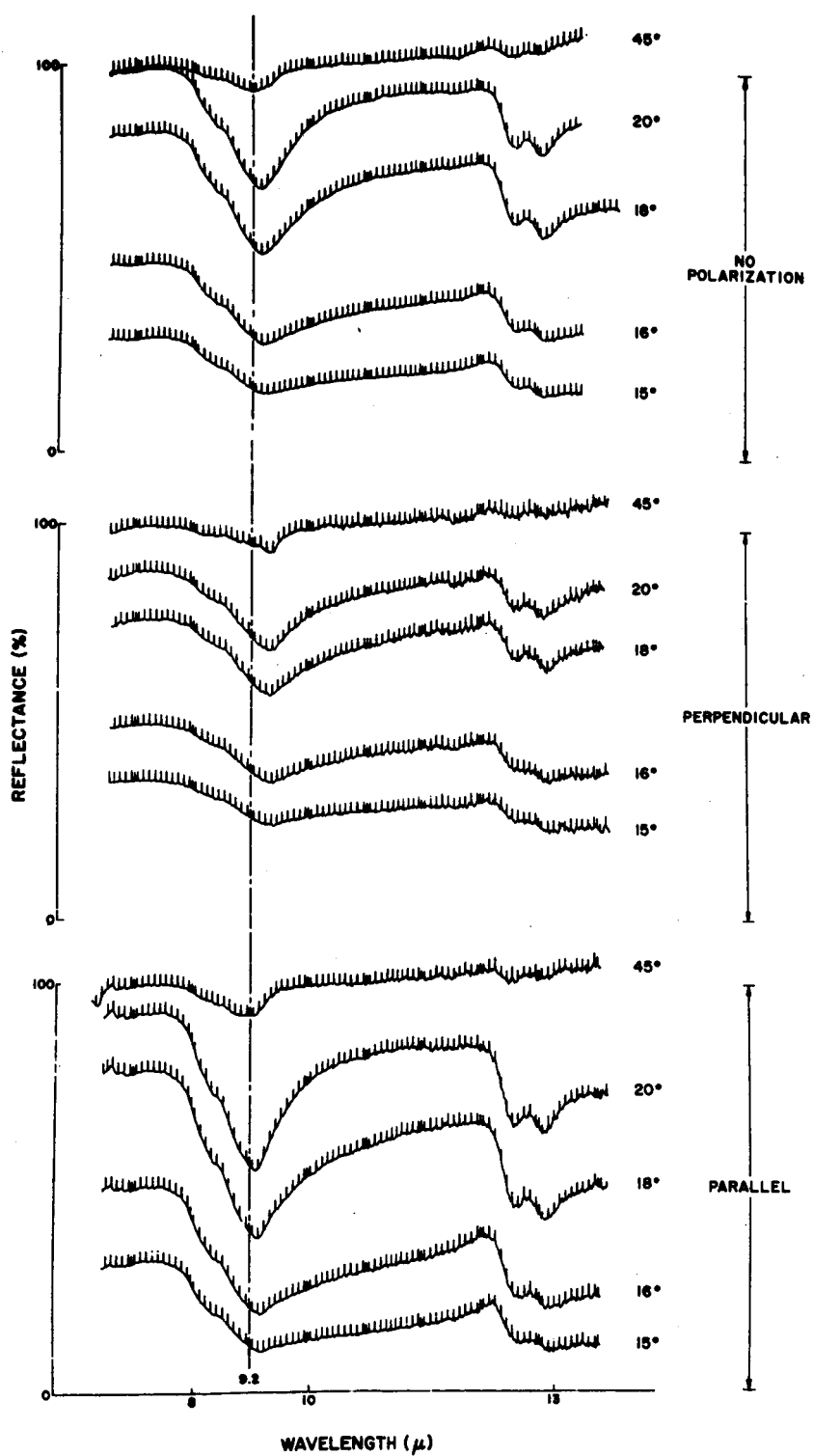


Figure 12: Internal Reflection Spectra of 0-3.5  $\mu$  Powdered Quartz Fraction Using Various Angles-of-Incidence, Ge Hemicylinder, and Different Polarizations.



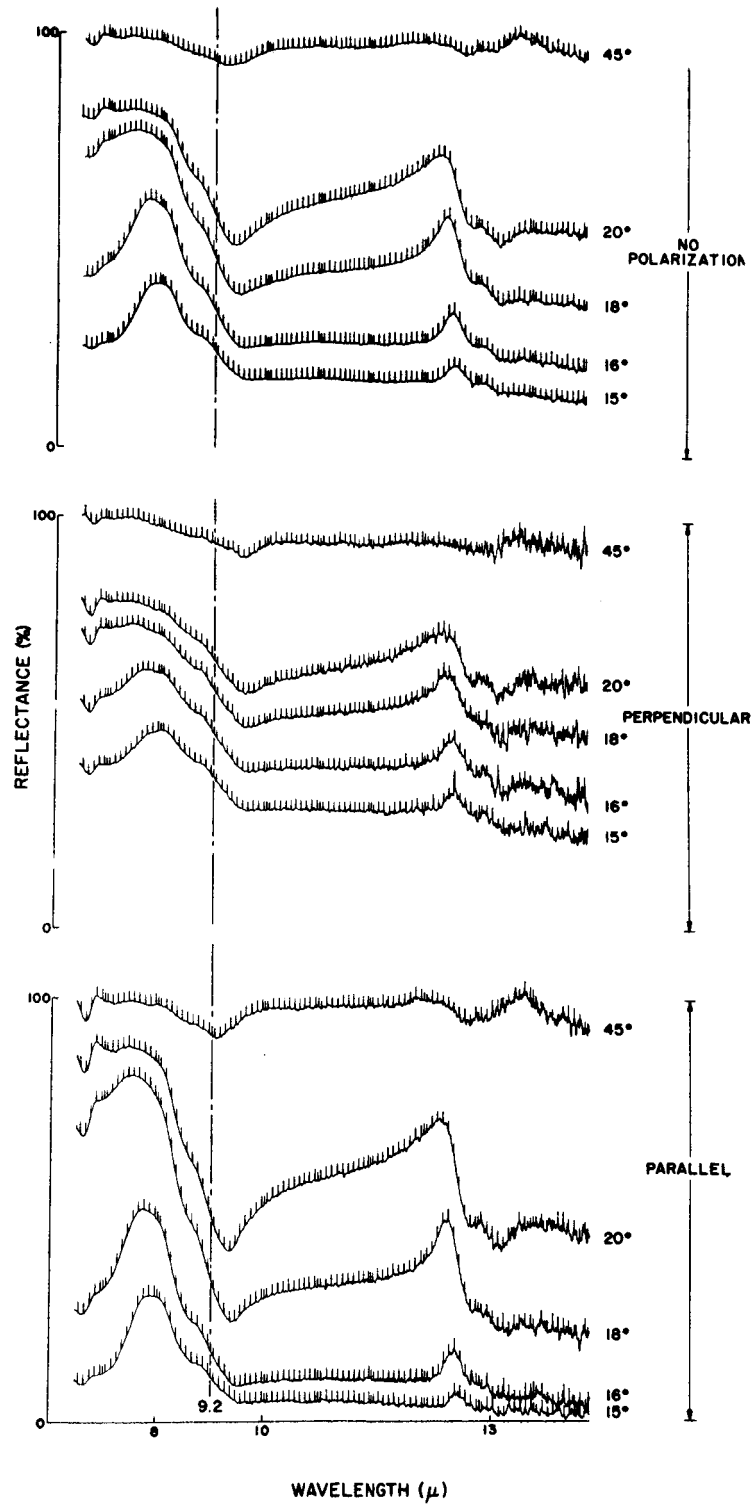


Figure 13: Internal Reflection Spectra of 0-3.5  $\mu$  Powdered Quartz Fraction Using Various Angles-of-Incidence, GaAs Hemicylinder and Different Polarizations.

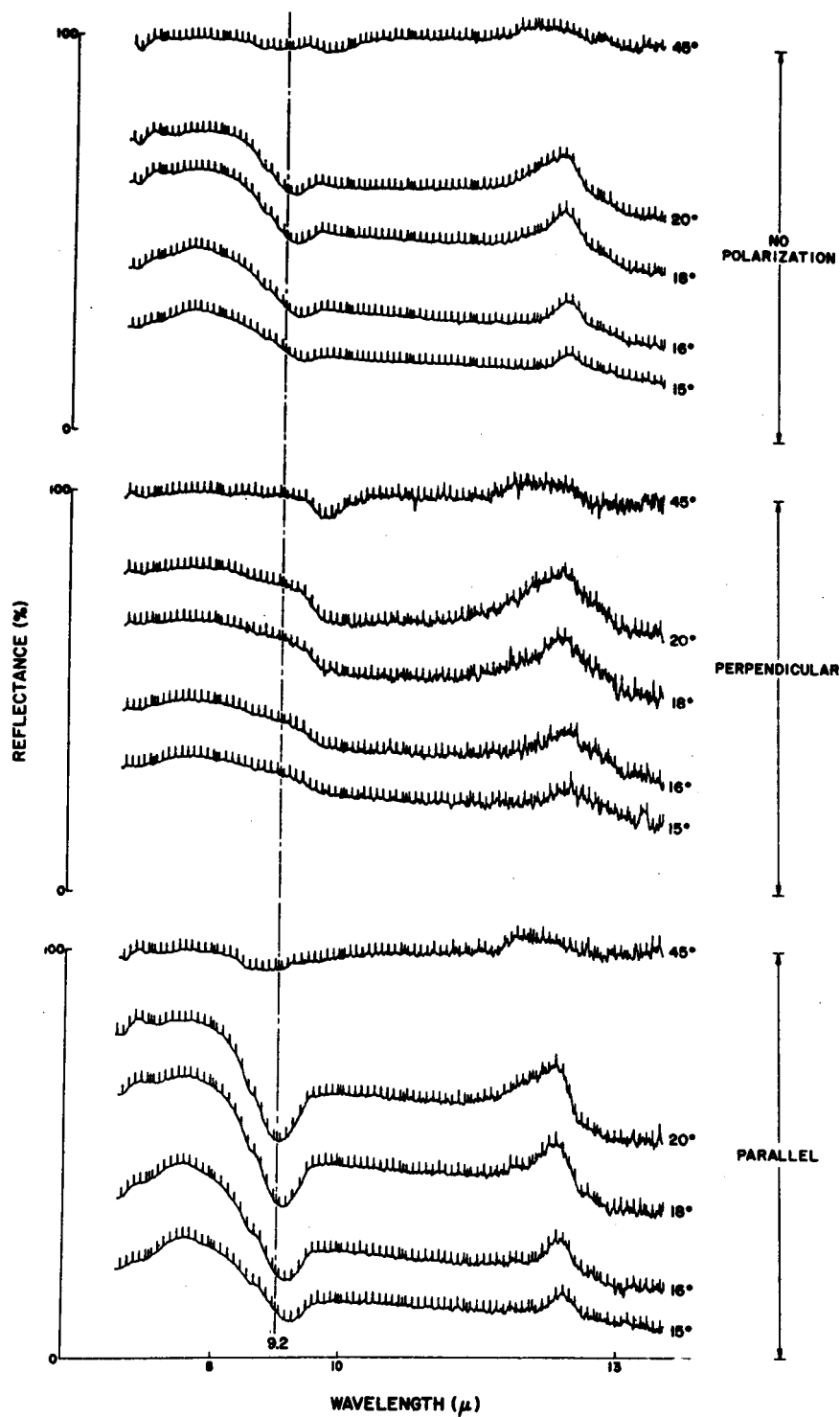


Figure 14: Internal Reflection Spectra of 10-20 $\mu$  Powdered Quartz Fraction Using Various Angles-of-Incidence, Ge Hemicylinder and Different Polarizations.

### 3.6 Reflection Mechanism at Surface/Powder Interface

The powdered quartz data was analyzed; our observations and interpretations are as follows:

#### 3.6.1 Observations

a) Interaction in Non-Absorbing Regions. In the non-absorbing regions (where the index of refraction  $n$  is much greater than the extinction coefficient  $k$ , in the complex refractive index  $\hat{n} = n - ik$ ) little or no change in the reflectance with change in particle size or change in wavelength was observed for both parallel and perpendicular polarization, at angles-of-incidence of  $30^\circ$ ,  $45^\circ$  and  $60^\circ$ . The accuracy of these results is considerably better at the shorter wavelengths (2 to  $5\mu$ ) than at the longer wavelengths (greater than  $10\mu$ ), principally because of the lower noise levels. This is due to the higher infrared power available at the shorter wavelengths.

#### b) Interaction in Absorbing Regions.

- Internal reflection spectra can be obtained regardless of particle size.
- Contrast of spectra decreases with increase in angle-of-incidence, with increase in refractive index of the internal reflection element and with increase in the particle size of the powder.
- The spectra for perpendicular polarization show a displacement of the absorption bands, with respect to the 9.2 micron reference, towards longer wavelengths. These displacements do not seem to be strongly dependent on particle size, however, displacements are present in all powdered quartz fractions.
- The spectra for parallel polarization show a displacement of the absorption bands, with respect to the 9.2 micron reference line, towards shorter wavelengths. Except for the 3.5 micron fraction, these displacements depend strongly on particle size. As the particle size increases, the bands become further displaced towards the shorter wavelengths. Such a large displacement or change with particle size was not observed for the band at  $8.5\mu$ .

### 3.6.2 Interpretations

a) Non-Absorbing Regions. The most important observation in the course of this work was the further confirmation of little or no scattering in non-absorbing regions (at  $\theta = 45^\circ$ ) by particulate matter on the surface of the internal reflection element - for powdered specimens whose diameters were smaller, equal to and greater than the wavelength of the light used.

Similar observations were also made at angles-of-incidence of  $30^\circ$  and  $60^\circ$ , using germanium internal reflection plates. The significance of these observations is that optical spectra can be recorded of particulate matter by means of internal reflection. Furthermore, no sample preparation is required, i.e., no nulls, pellets, or particle sizing. It should be recalled that because of excessive light scattering, useful spectra cannot be obtained via transmission techniques unless this scattering is considerably reduced. This scattering can be reduced considerably by employing very fine particles or by embedding the powder in a matrix of the same refractive index. In the latter case, a matrix having a suitable refractive index cannot always be found, and it is not always possible to match the indices over the entire wavelength range.

Although considerable thought and discussion has been devoted to this apparent lack of scattering, we can offer no theoretical explanation for this observation. Scattering, it should be recalled, is extremely involved and only the simplest problems involving scattering have been solved.

A mathematical model that could be used for interpreting the small or negligible loss in reflectance in the non-absorbing regions would involve the following: examination of the scattering from homogeneous, isotropic spherical particles, using an incident wave having an exponentially decreasing amplitude. The formal mathematics are similar to Mie's solution (Ref. 4) of a rigorous solution for the diffraction of a plane monochromatic wave by a homogeneous sphere of any composition and size in a homogeneous medium. The only change is that the plane monochromatic wave has an exponentially decreasing amplitude in the direction of the normal to the surface of the internal reflection element. This theoretical analysis is applicable to both (1) the wave component traveling tangentially to the surface of the internal reflection element and (2) the wave component traveling normal to this surface. The analysis may be extended to the case where the spherical particle has been replaced by a cylindrical particle of infinite length.

The extension of the solution for any number of spherical or cylindrical particles is based on the assumption that there are no coherent phase relations between the light scattered by the individual particles.

b) Absorbing Regions. The second most important observation is that spectra can be obtained regardless of particle size. This is not so in transmission, where, if the particles are too large, no useful spectra can be obtained because any light striking the particle is completely absorbed (in the absorbing regions).

The decrease in contrast of the internal reflection spectra with increase in particle size is explained by the decrease in packing fraction. The decrease in contrast of the spectra with increase of refractive index of the internal reflection element and with increase in the angle-of-incidence is also completely understood (Ref. 5). This is explained by the change in interaction of the evanescent wave with the absorbing medium with change in angle-of-incidence and change in refractive index.

In the previous work on quartz-kaolinite mixtures, the spectra resembled that obtained via transmission and was, except for contrast, substantially independent of particle size. In other work at Philips Laboratories, the spectra of isotropic material - except for contrast - were found to be independent of polarization. This difference in contrast can be explained in terms of the interaction mechanisms for different polarizations (Ref. 5). In the present work, the spectra were found to be dependent both on polarization and to some extent on the particle size. We have no theoretical explanation for this. However, we wish to point out some of the difficulties involved. Firstly, for an undamped material like quartz, very large changes in refractive index (e.g., 0 to 7) and in absorption coefficient (zero to metallic) occur in the vicinity of absorption bands. Also, quartz is birefringent; and, in the present measurements, we are dealing with particulate matter. All of these factors make the problem of precisely explaining the results extremely complicated. Furthermore, it should be realized that the condition for total internal reflection, where the angle-of-incidence exceeds the critical angle, cannot be maintained on a material like quartz because of the large changes in refractive index. For a high index, internal reflection plate material like germanium, the index  $n$  equals 4; yet for quartz,  $n$  changes from 0 to more than 7. Also, the low refractive index and high absorption coefficient for quartz make the reflection metallic in some spectral regions.

## PHILIPS LABORATORIES

In an attempt to interpret the spectra of the powdered quartz, internal reflection measurements were made on a solid oriented quartz plate (see Figures 15,16). The drastic differences in the spectra for perpendicular and parallel polarization should be noted, as well as some similarities of the spectra of the solid to those of the powders. For a complex refractive index and birefringent material, we have no doubt that these measurements on the solid quartz plate can be explained by Fresnel's equations. In our opinion, measurements of this type should be continued and understood before attempting to understand the results for particulate matter like quartz.

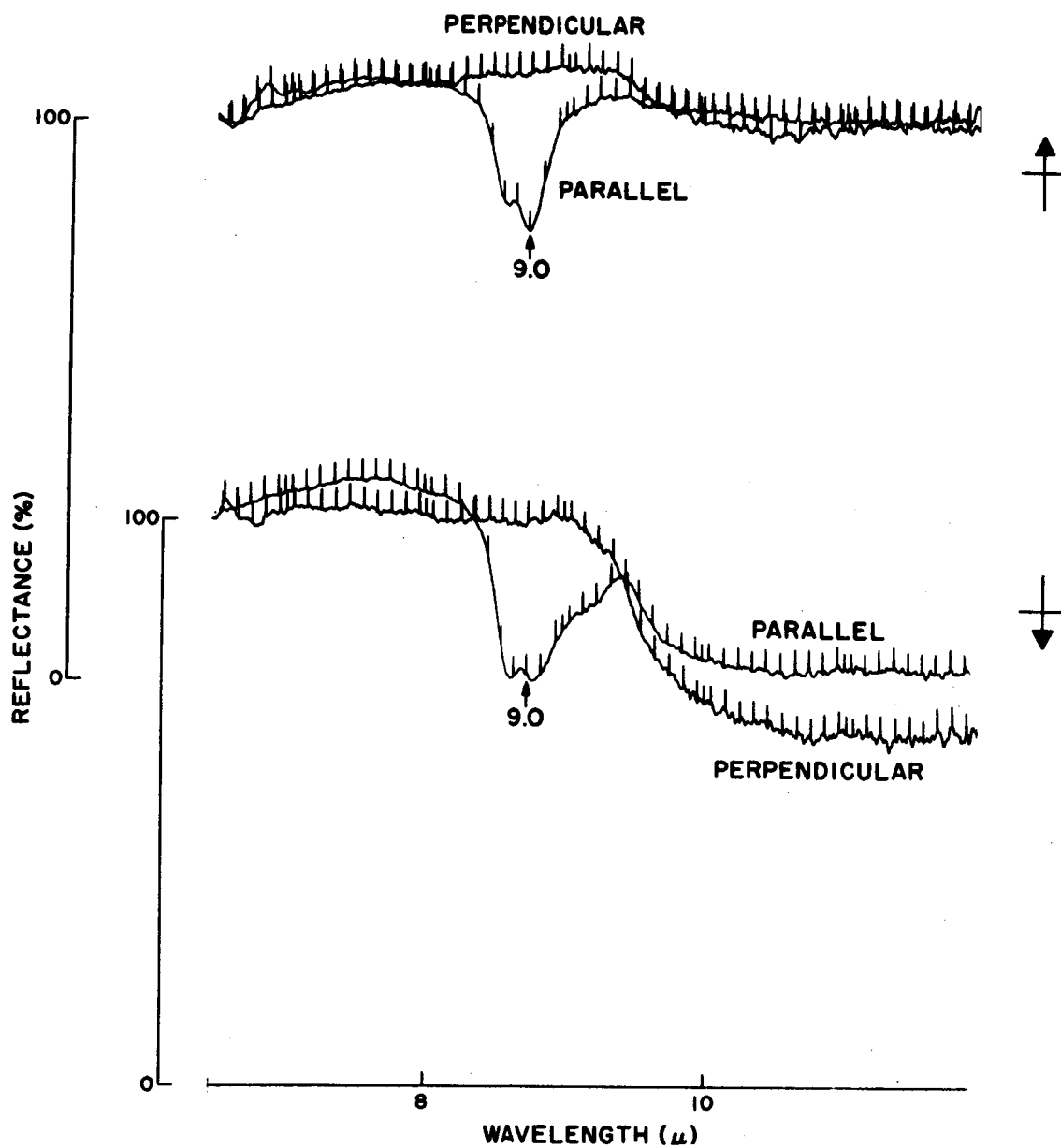


Figure 15: Internal Reflection Spectra of Solid Quartz Crystal (A-T Cut) Using  $\theta = 45^\circ$ , KRS-5 Hemicylinder, Perpendicular and Parallel Polarization, and Two Orientations of the Optical Axis With Respect to the Incident Light.

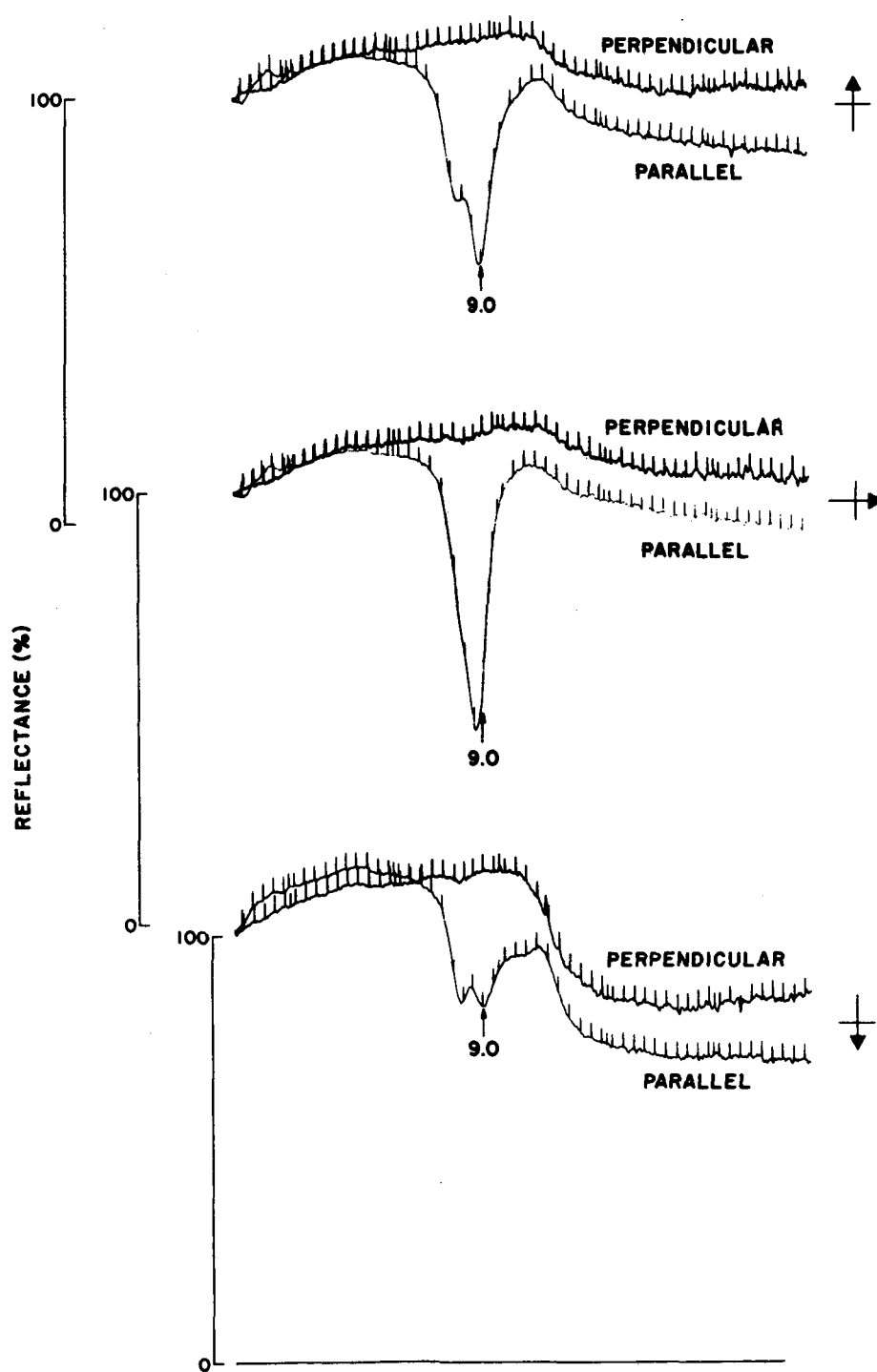


Figure 16: Internal Reflection Spectra of Solid Quartz Crystal (A-T Cut) Using  $\theta = 35^\circ$ , KRS-5 Hemicylinder, Perpendicular and Parallel Polarization, and Three Orientations of the Optical Axis With Respect to the Incident Light.



### 3.7 Methods for Quantitative Measurements

There is no fundamental problem in making quantitative measurements via Internal Reflection Spectroscopy. For a complex refractive index, the degree of interaction of the evanescent wave with the rarer medium is expressed precisely by Fresnel's equations. Uniform physical contact between the internal reflection element and the rarer medium is assumed, and such contact is easily achieved for liquids and pliable materials. For solids and powders, on the other hand, good uniform contact is not readily achieved. Therefore, in these cases, before quantitative measurements can be made, the actual or effective area of contact between the internal reflection element and the sample material must be determined.

A method is proposed for determining this contact area for solids and powders. This method is based on a measurement of the reflectivity at the principal angle in wavelength regions where the sample material is non-absorbing. It should be recalled that the reflection coefficient for parallel polarization is zero at the principal angle. Therefore, any deviation of the reflection coefficient from zero will provide a measure of the effective area of contact. We stress "effective" because actual physical contact is not necessary for obtaining interaction with the evanescent wave - it is only necessary to bring the material to within a penetration depth. The smaller the separation, the greater will be the interaction. Since the penetration depth is directly proportional to wavelength, the effective area of contact will increase as the wavelength increases. Therefore, the contact area determined in this way must be measured in the wavelength region where the other quantitative measurements are being conducted.

### 3.8 Comments on Measurement of Optical Constants via Internal Reflection Spectroscopy

Internal Reflection Spectroscopy has been successfully employed in a number of cases (Refs. 6,7,8) for the measurement of optical constants. It has some important advantages over conventional transmission and reflection techniques in this application. Firstly, the absence of interference fringes simplifies the intensity measurements. Secondly, the recorded spectra may be made sensitive to either changes in absorption coefficient or changes in refractive index. This is evident in Figure 17 which clearly shows that measurements made at angles-of-incidence well above the critical angle tend to resemble the absorption coefficient, while measurements made just below the critical angle tend to resemble the mirror image of the dispersion in the refractive index. Two such measurements, judiciously chosen, can with the aid of Fresnel's equations be combined to yield accurate values of the optical constants. The optical constants might also be determined from two measurements made with different polarizations.

Simon (Refs. 9,10) discussed a two-angle method for the measurement of the optical constants of materials such as quartz. His technique employed external reflection and is similar to the present approach in that the index of refraction is below unity in certain spectral regions, thus establishing the condition for total reflection without the use of a prism of high index in these regions. In fact, for materials such as quartz, not much is gained by employing internal reflection for the measurement of optical constants, since the refractive index varies too much and total reflection cannot be maintained throughout the absorption band for any angle-of-incidence.

For measuring the optical constants of powdered quartz, via internal reflection, there are a number of problems. One was just mentioned in the previous paragraph; viz., that with large variations in both  $n$  and  $k$ , it is questionable whether anything is gained by employing internal reflection over conventional external reflection. It should be noted, however, that dispersion-type spectra can be obtained by making measurements near the critical angle (see Figures 12,13 and 14). Other problems have to do with the particulate nature of the sample. Firstly, contact area must be precisely determined; this might be done as described in the section on quantitative measurements. Secondly, the spectra of the powdered quartz depends on the particle size and polarization which, as discussed earlier, probably is due to the large variations in the optical constants and the birefringence of quartz (Ref. 11).

A comparison of the spectra (see Figures 12,13) of the 0-3.5 $\mu$  quartz fraction using a germanium hemicylinder ( $n = 4$ ) and a gallium arsenide hemicylinder ( $n = 3.4$ ) illustrates the effect that the material of the internal reflection element has upon sensitivity. The gallium arsenide spectra show an increase in reflectance for angles-of-incidence below the critical angle of quartz, for the 9 micron region. A similar phenomenon is not noticed in the spectra obtained with the germanium element. This is not surprising when one considers the large changes in the refractive index of quartz near 9 microns.

In order to compare the spectra of powdered quartz to the spectra of solid crystalline quartz for internal reflection spectroscopy, an A-T cut of quartz was used. Two angles-of-incidence ( $45^\circ$ ,  $35^\circ$ ) were used with a KRS-5 hemicylinder and different states of polarization. For an A-T cut, the optic axis of the crystal makes an acute angle to the normal of the surface; the plane of the optic axis is defined as the plane containing the optic axis and the normal to the surface of the crystal.

Figure 15 illustrates spectra of A-T cut quartz using a KRS-5 hemicylinder,  $45^\circ$  angle-of-incidence, different states of polarization, and different orientations of the optical plane with respect to the plane-of-incidence (symbolically shown by the orientation of the arrow).

Figure 16 illustrates spectra of A-T cut quartz using a KRS-5 hemicylinder,  $35^\circ$  angle-of-incidence, different states of polarization, and different orientations of the optical plane with respect to the plane-of-incidence.

The principal feature of Figures 15 and 16 is that the perpendicular polarization spectra show no minima in the region of 9 microns. This absence in both the powdered quartz and crystalline quartz must be attributed to the crystalline nature of quartz and not to the form of the quartz, i.e., powder and solid.

We wish to draw attention to a recent publication (Ref. 12) concerning the problem of measuring the optical constants of powders. The article points out that if very fine powders are pressed to form a very smooth surface, then conventional reflection measurements can be made. This approach should also be suitable for internal reflection techniques, and should thereby eliminate the need for measuring the packing fraction.

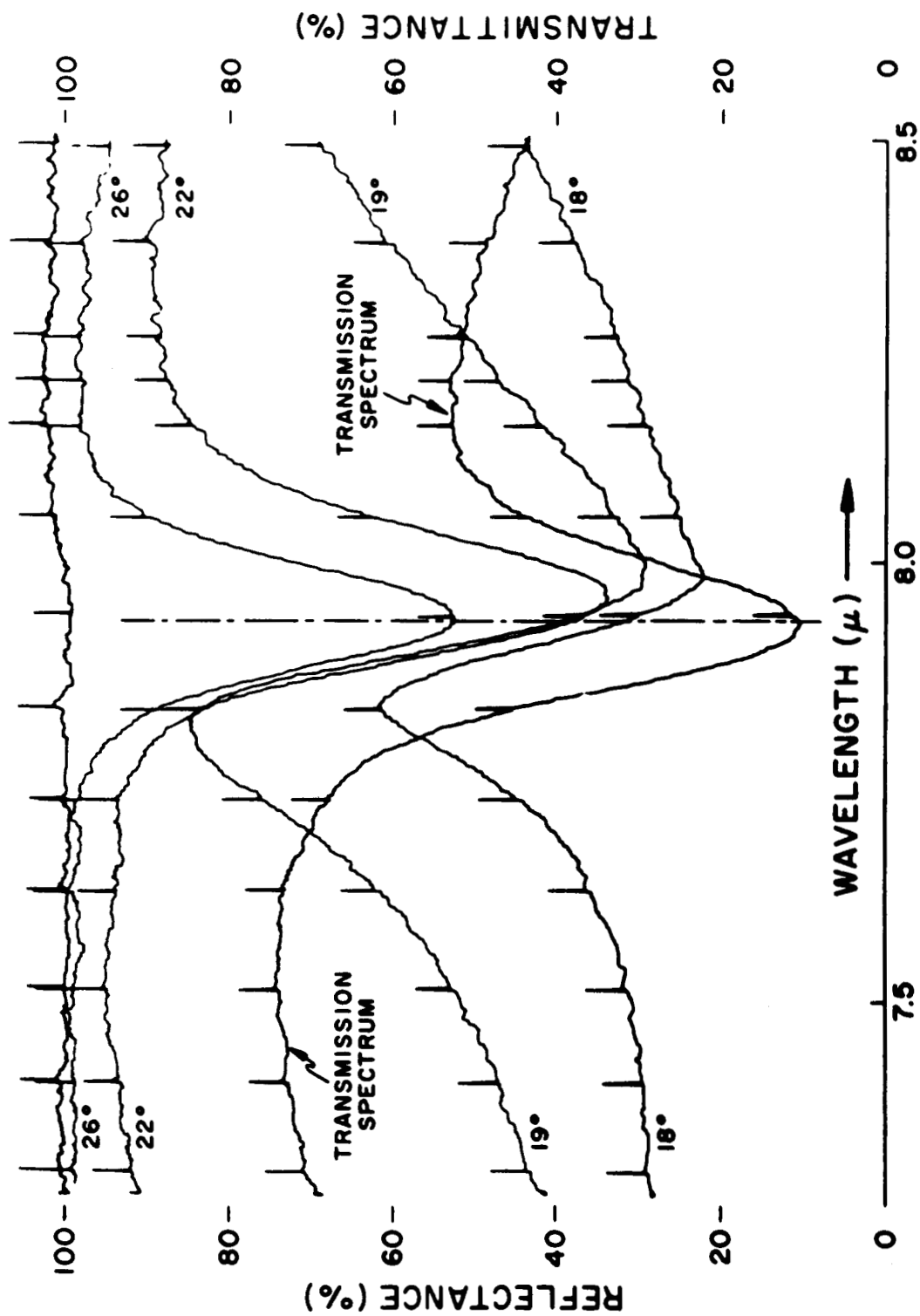


Figure 17: Internal Reflection Spectra of  $7.9\mu$  Absorption Band of Silicone Lubricant vs Angle-of-Incidence

### 3.9 Instrument Design Approach

For study of powdered samples (rocks and minerals), the instrumentation as outlined in this report has proved satisfactory. The ease with which the internal reflection technique can be employed is determined by the spectrometer design; therefore, modification of a spectrometer for this purpose requires careful consideration.

The vertical or horizontal double-pass plates are desirable since one end of the plate is free and can be dipped directly into the powder. Pertaining to the optical layout, the internal reflection elements should be readily accessible so that the sample can easily be placed in contact with the element. Adequate space should also be provided for accessories such as polarizers, etc. Commercial attachments for conventional spectrometers do not, in general, meet these requirements. The optical layout we have developed (see Figure 5) meets these requirements; and, in addition, enables the angle-of-incidence to be varied over a wide range, thereby enhancing the versatility of the instrument.

The incorporation of 90° out-of-phase chopping and signal detection eliminates the need for optical nulls and programmed slit drives. This design feature has simplified the construction of the present laboratory instrument. Also, the signal processing presents the reflectance information in a form which, when recorded, requires no additional computation. Although careful alignment of the two light beams is required, once aligned, the instrument has a  $\pm 0.5\%$  stability.

## PHILIPS LABORATORIES

### 3.10 Internal Reflection Spectra of NASA-Supplied Powdered Rocks

Internal reflection spectra (see Figures 18 to 33) were obtained for the fourteen (14) powdered rock samples supplied by NASA. The particle size of the samples was 200 mesh. A listing of these rocks and their origins are shown below.

<u>Powder Sample</u>	<u>Code Name</u>	<u>Origin</u>
(1) Andesite	AGV-1	Guano Valley, Oregon
(2) Basalt	BCR-1	Columbia River, Oregon
(3) Dunite	DTS-1	Twin Sisters, Wash.
(4) Westerly Granite	G-2	
(5) Granodiorite	GSP-1	Silver Plume, Colorado
(6) Peridotite	PCC-1	Cazadero Quadrangle Sonoma County, Calif.
(7) Augite	R 15162	Templeton, Quebec, Canada
(8) Albite	117 741	Weiant Quarry, Cecil County, Maryland
(9) Bronzite	82 436	Webster, North Carolina
(10) Fayalite	R 3517	Rockport, Mass.
(11) Hedenbergite	R 7584	Calera Mine, near Guerrerna, Chihuahua, Mexico
(12) Labradorite	R 15163	Lake St. John, Quebec, Canada
(13) Olivine	117 280	Camperdown, Victoria, Australia
(14) Orthoclase	R 7508	Striegau, Silesia, Germany

Samples (1) through (6) were received courtesy of M.W. Molloy of NASA from R.J.P. Lyon of Stanford University and F.J. Flanagan of the U. S. Geological Survey. Samples (7) through (14) were received courtesy of M.W. Molloy from E.P. Henderson of the U. S. National Museum.

Figures 18 to 31 are the individual spectra of the 14 powdered rocks, using a fixed 45° double-pass KRS-5 plate, and Figure 32 shows the spectra of powdered Fayalite for two polarizations. Figure 33 is a composite showing the spectra of 6 of the 14 samples, using a 45° double-pass germanium plate.

# PHILIPS LABORATORIES

Where possible, the spectra of the powdered rocks are grouped according to the structure class of the silicates and to their series within a class. This is shown in the following table.

<u>Figure No.</u>	<u>Sample</u>	<u>Structure Class</u>	
18	Orthoclase	Framework	
19	[ Albite	↓	
20			Andesite
21			Labradorite
22	[ Augite	Single-Chain Silicates	
23		Hedenbergite	
24		Bronzite	
25	[ Olivine	↓	
26			Dunite
27			Fayalite
28	Peridotite	SiO <sub>4</sub> tetrahedron	
29	Basalt		
30	[ Granodiorite		↓
31			

The powder was introduced to the sampling surfaces of the internal reflection plate by first inserting the plate into a container which was then filled with the powder. Each of the two sampling surfaces of the plate were 28mm x 25mm; plate thickness was 2mm. There was a total of approximately 28 reflections, 14 per side. The powder was lightly packed by applying pressure from the open end of the container.

The spectra taken with the germanium plate (see Figure 33) were noticeably weaker than those obtained with the KRS-5 plate. Heavier packing of the powder did not improve the spectra obtained with the germanium plate. This difference in intensity between the spectra obtained with the KRS-5 plates and those obtained with germanium plates is due to the difference in index of refraction of the plates, and therefore a change in strength of interaction (Ref. 5). It should be noted that the KRS-5 plates are susceptible to surface scratches and therefore could only be used for 2 or 3 samples, after which the surfaces had to be refinished.

## PHILIPS LABORATORIES

The spectra of powdered Albite and Augite (see Figures 19,22) each show comparisons of the transmission technique (Refs. 13,14) and the internal reflection technique. Although there is a difference in the contrast of the spectra, there is close agreement in the positions of the minima. The contrast can, of course, be controlled by controlling the number of reflections, pressure and refractive index of the internal reflection element.

Transmission spectra, where available in published literature, were compared with the internal reflection spectra obtained of the NASA powdered rocks; there was close agreement in the positions of the minima. We wish to stress the fact that internal reflection has the advantage that particles of any size may be used and no sample preparation is required. It should be recalled that all of the present rock samples have particle sizes as large as 100 $\mu$ .

We wish to draw attention to the apparent scattering loss at the shorter wavelengths in the spectra recorded using KRS-5 plates. This is typical of KRS-5 reflection plates and is due to scattering associated with inadequate surface polish and not due to the presence of the powder on the surface. Also, since this material is rather soft, the surface polish deteriorates rather rapidly when used with powdered samples. For a much harder material like germanium, it is possible to obtain and maintain a much better surface polish. This is clearly demonstrated by the spectra shown in Figure 33.

Since the optical constants of these minerals are not known to us, and since these minerals contain silica, we wondered whether there would be a difference in the spectra for perpendicular and parallel polarization, as there was for quartz. The measurement was made on Fayalite (Figure 32). These spectra show a negligible variation in the positions of the minima for parallel and perpendicular polarization. In general, we expect the resonances to be more highly damped than those of quartz; and, as a result, no large variations in the optical constants, as in the case for quartz. Therefore, the complications that occur for pure quartz should not exist.



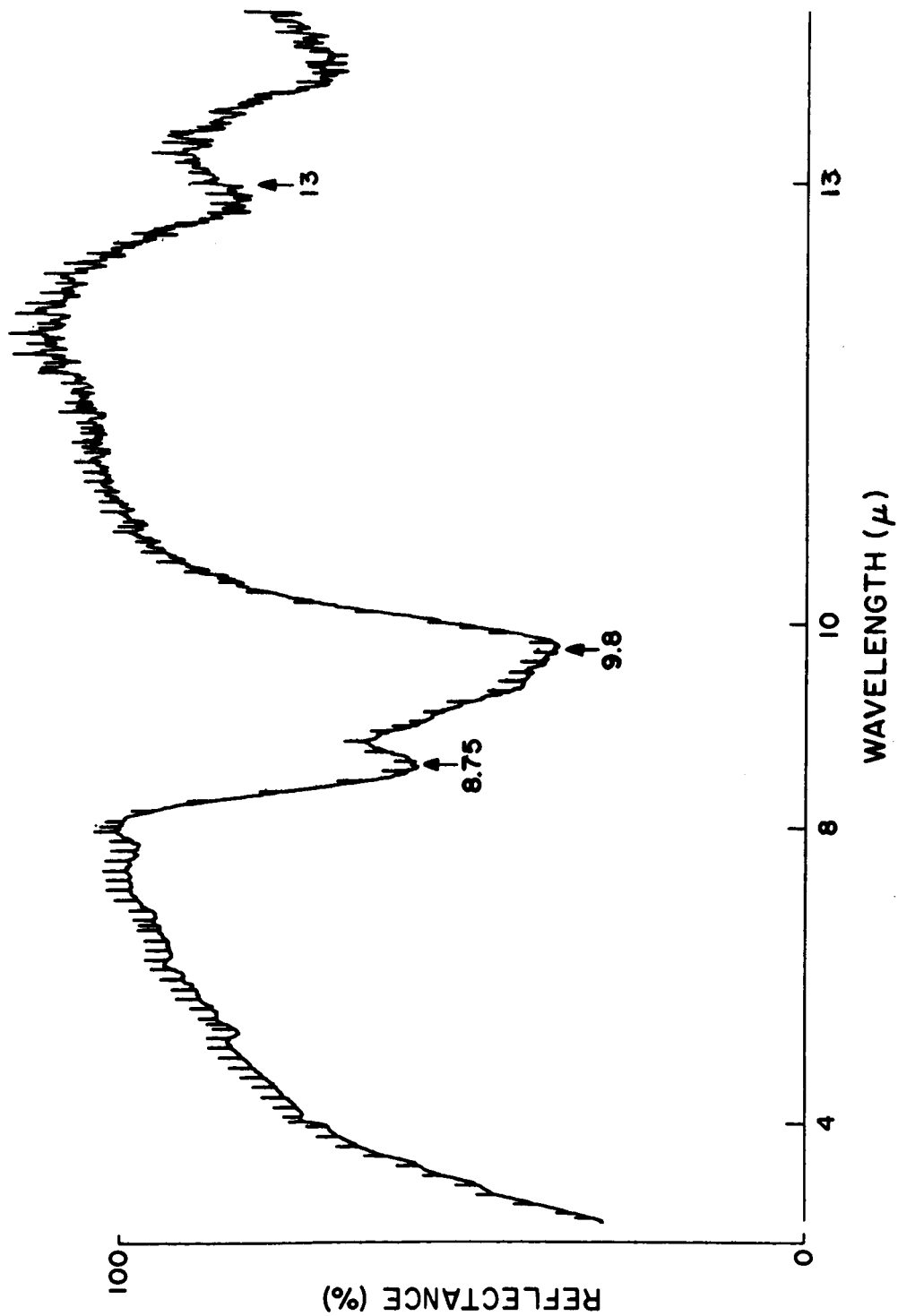
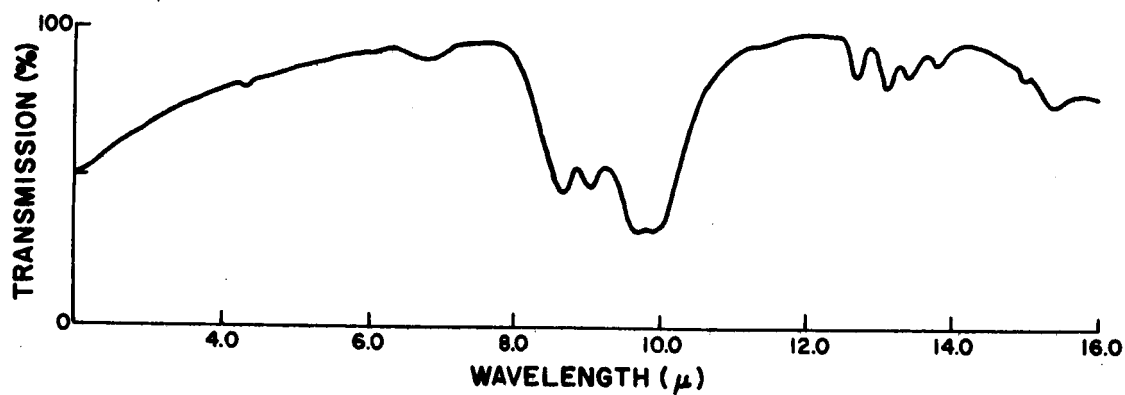
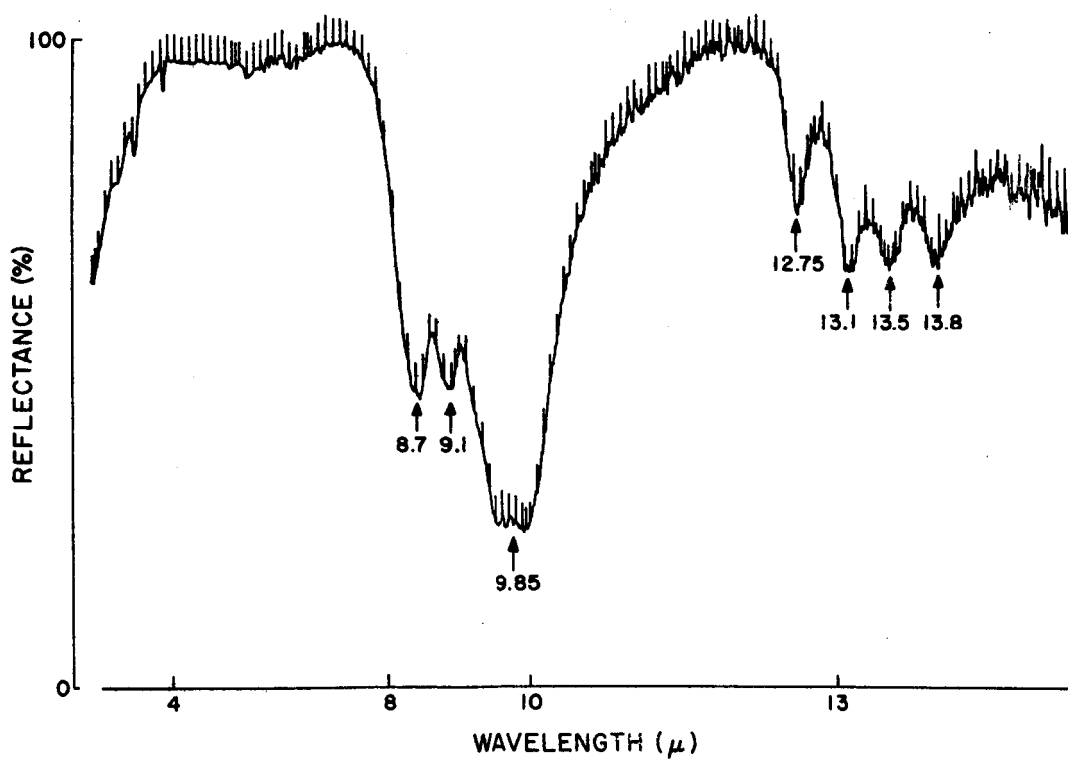


Figure 18: Internal Reflection Spectrum of Powdered Orthocase Using  $\theta = 45^\circ$  and KRS - 5 Plate.



a



b

Figure 19: Transmission and Internal Reflection Spectra ( $\theta = 45^\circ$ , KRS-5 Plate) of Powdered Albite.

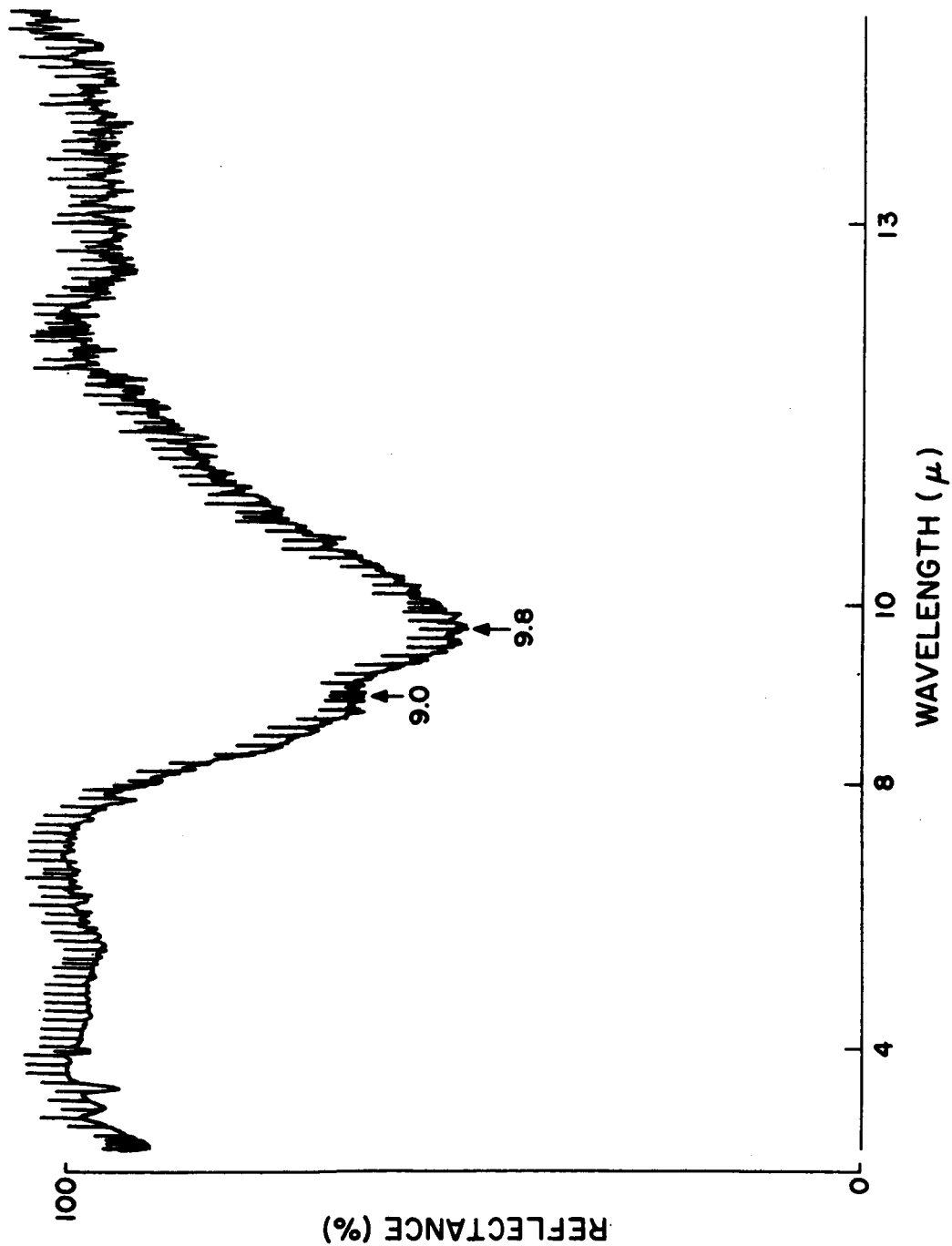


Figure 20: Internal Reflection Spectrum of Powdered Andesite (AGV-1) Using  $\theta = 45^\circ$  and KRS-5 Plate.

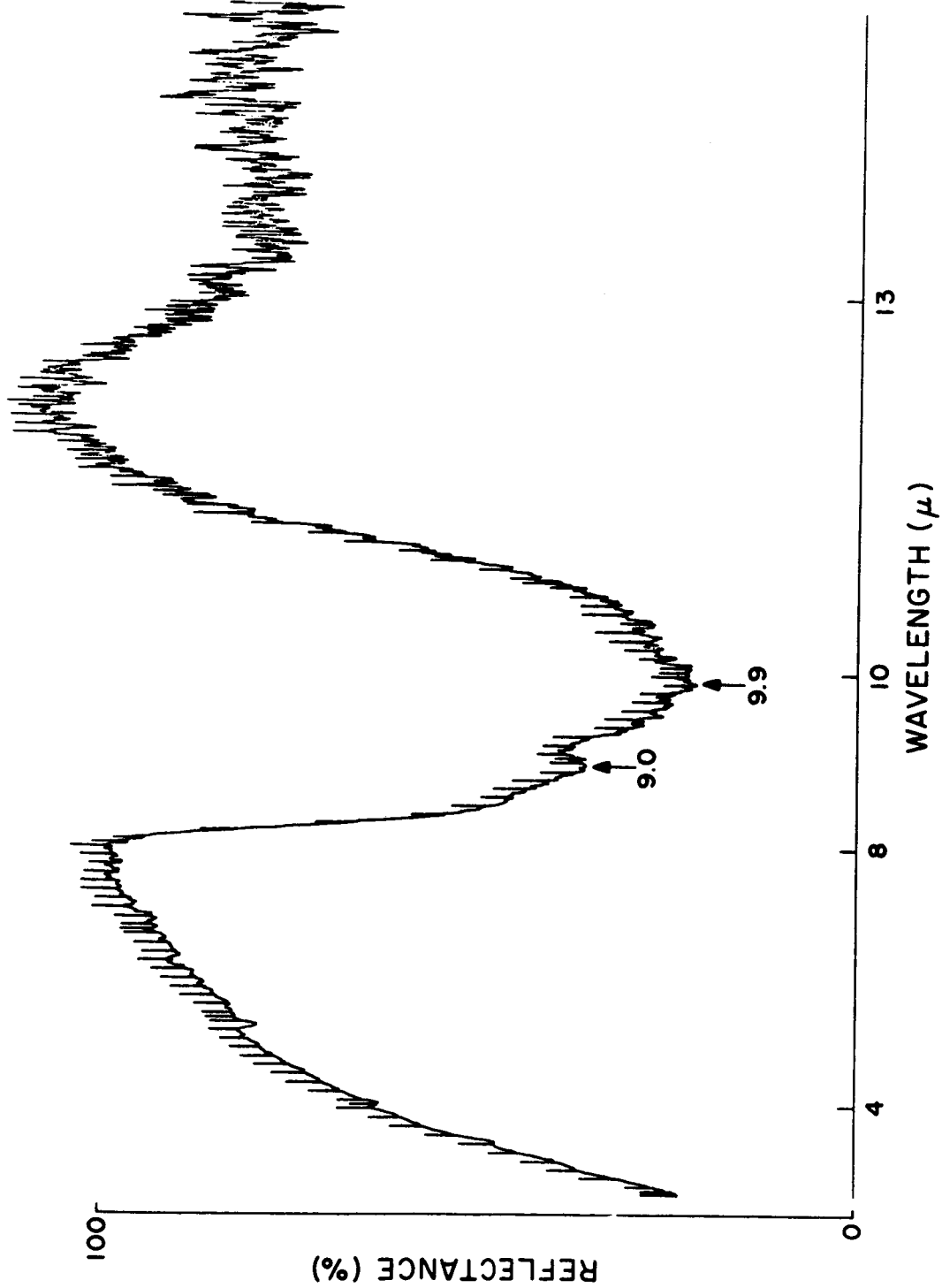
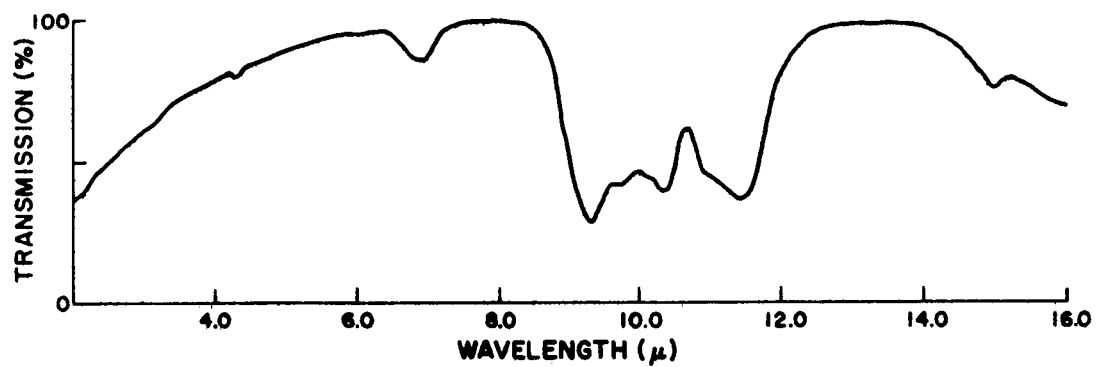
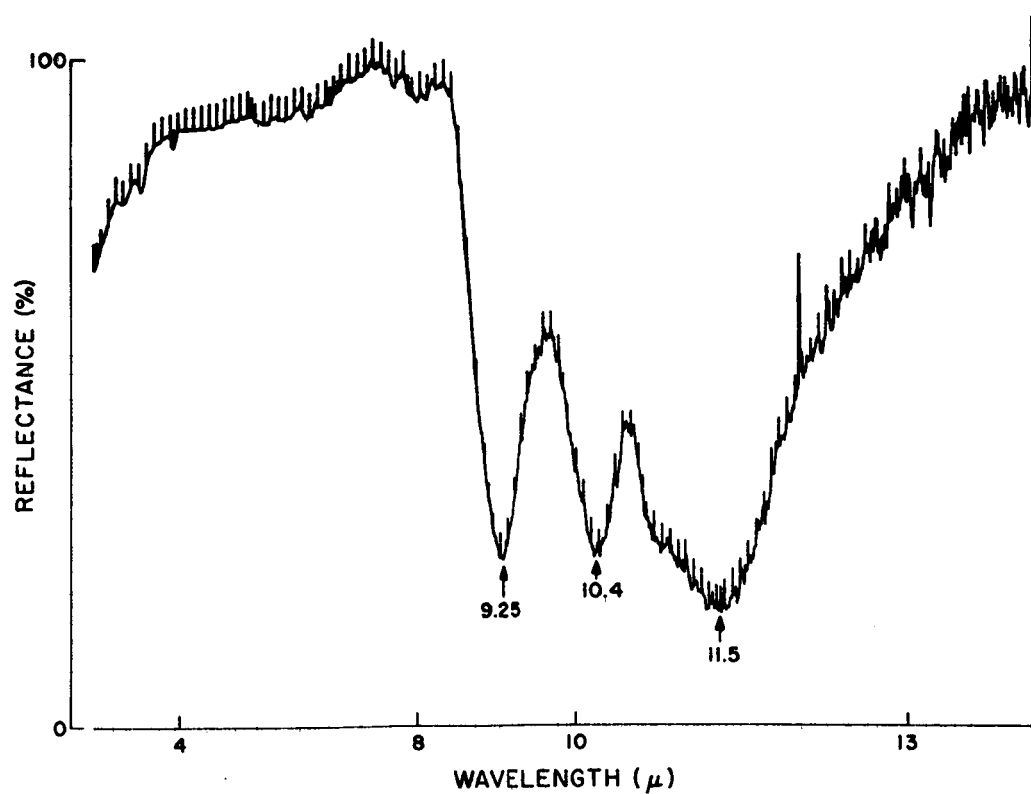


Figure 21. Internal Reflection Spectrum of Powdered Labradorite Using  $\theta = 45^\circ$  and KRS-5 Plate



a



b

Figure 22: Transmission and Internal Reflection Spectra ( $\theta = 45^\circ$ , KRS-5 Plate) of Powdered Augite.

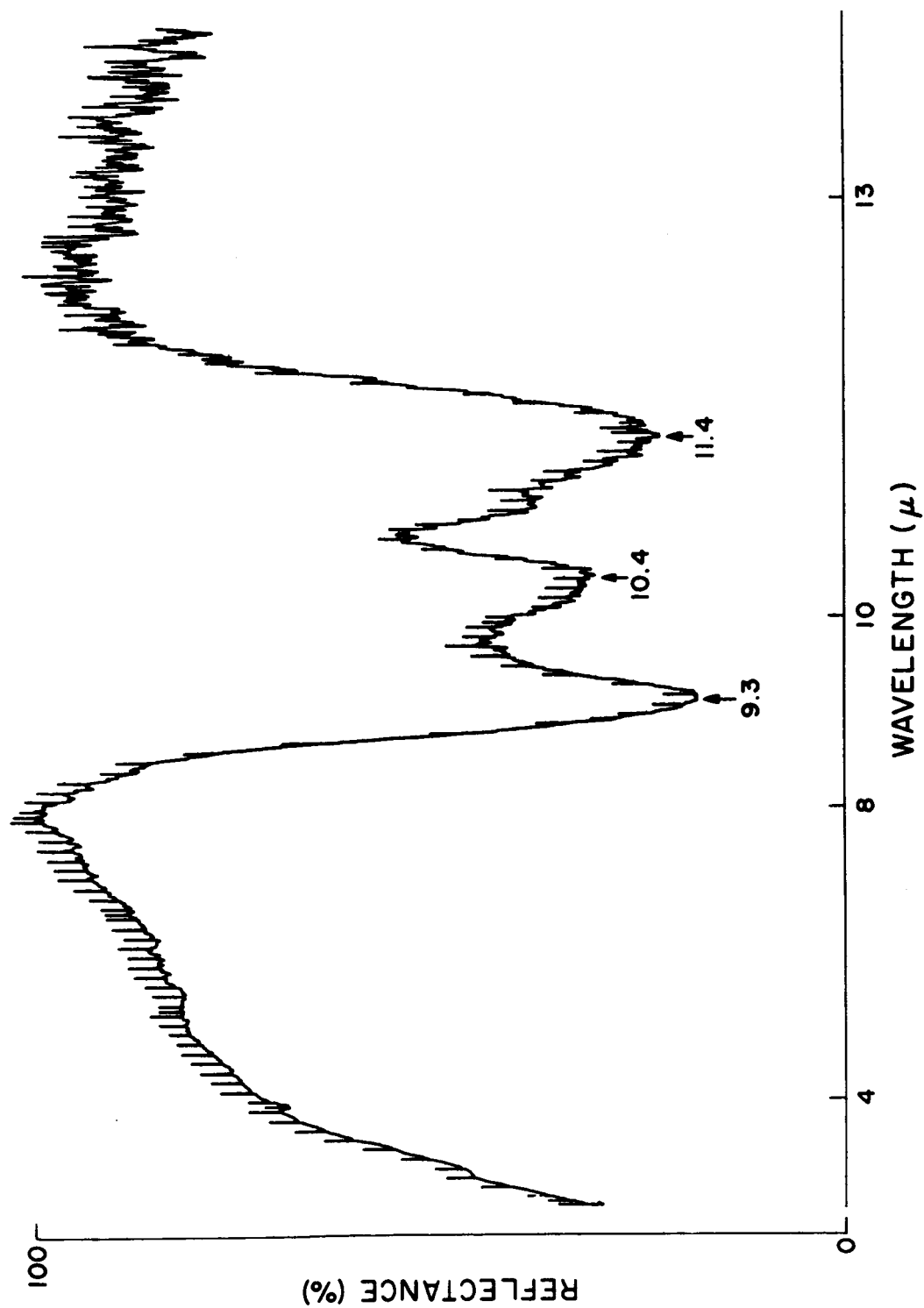


Figure 23: Internal Reflection Spectrum of Powdered Hedenbergite Using  $\theta = 45^\circ$  and KRS-5 Plate.

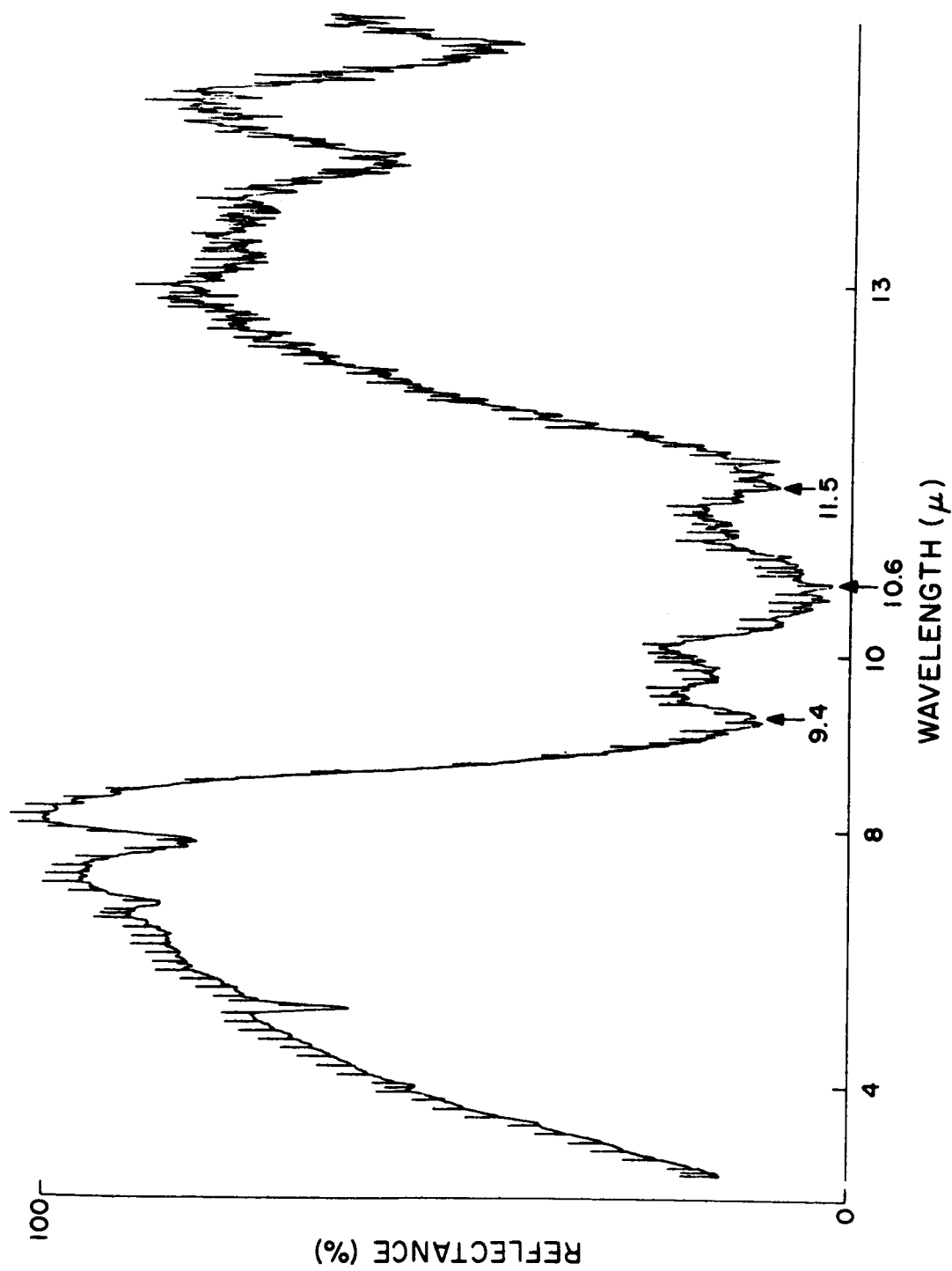


Figure 24: Internal Reflection Spectrum of Powdered Bronzite Using  $\theta = 45^\circ$  and KRS-5 Plate

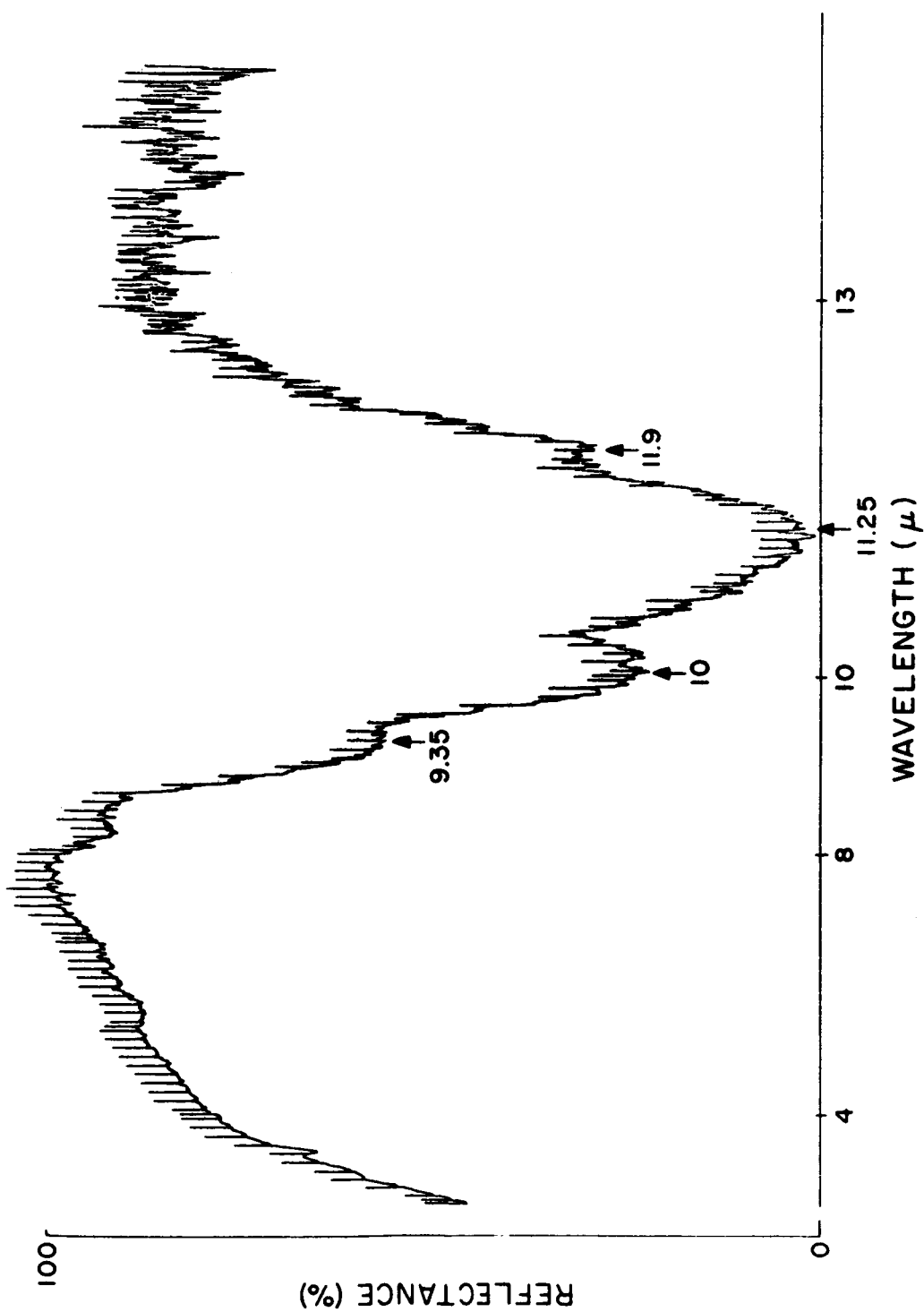


Figure 25: Internal Reflection Spectrum of Powdered Olivine Using  $\theta = 45^\circ$  and KRS-5 Plate.



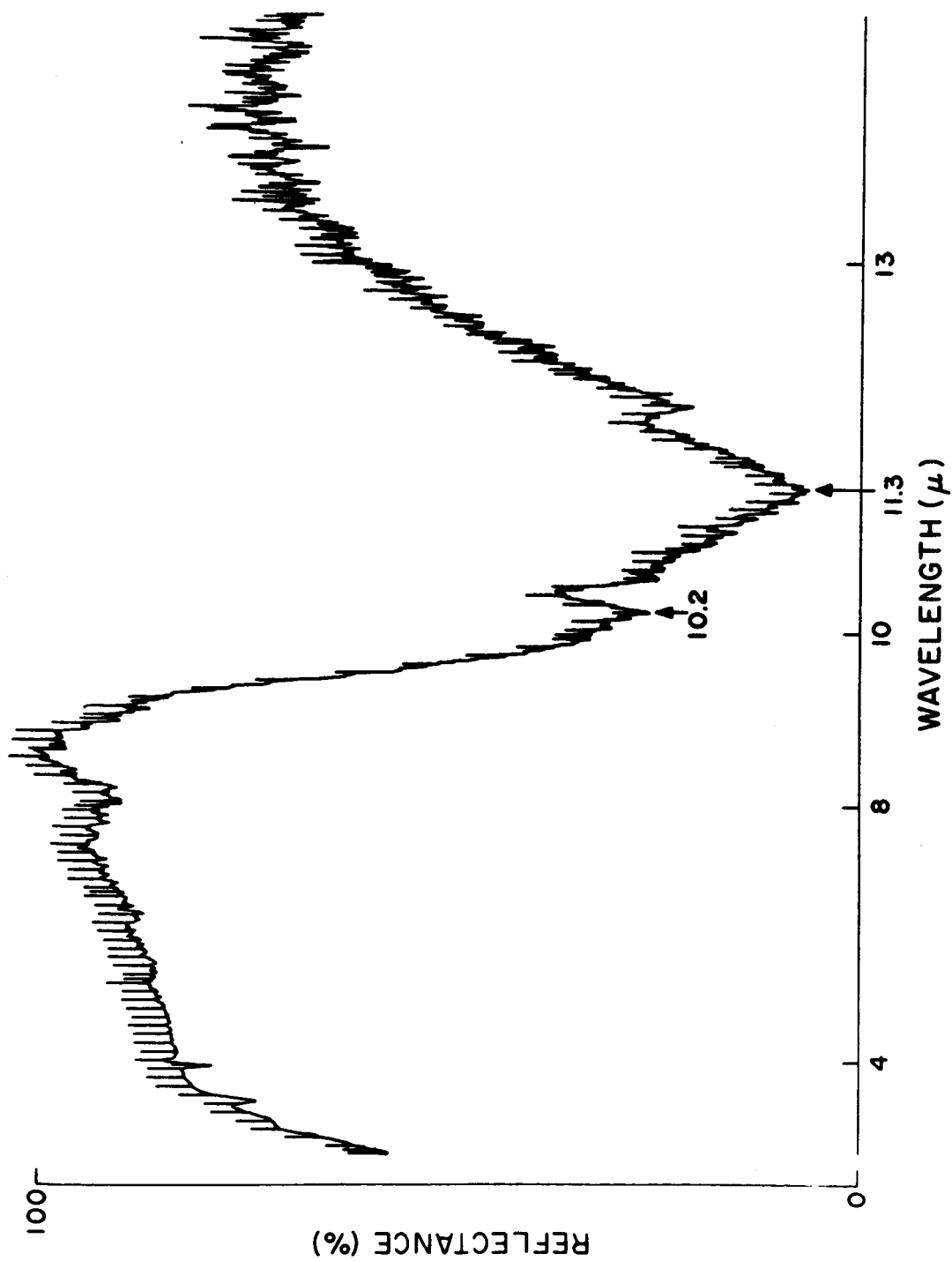


Figure 26: Internal Reflection Spectrum of Powdered Dunite (DTS-1) Using  $\theta = 45^\circ$  and KRS-5 Plate

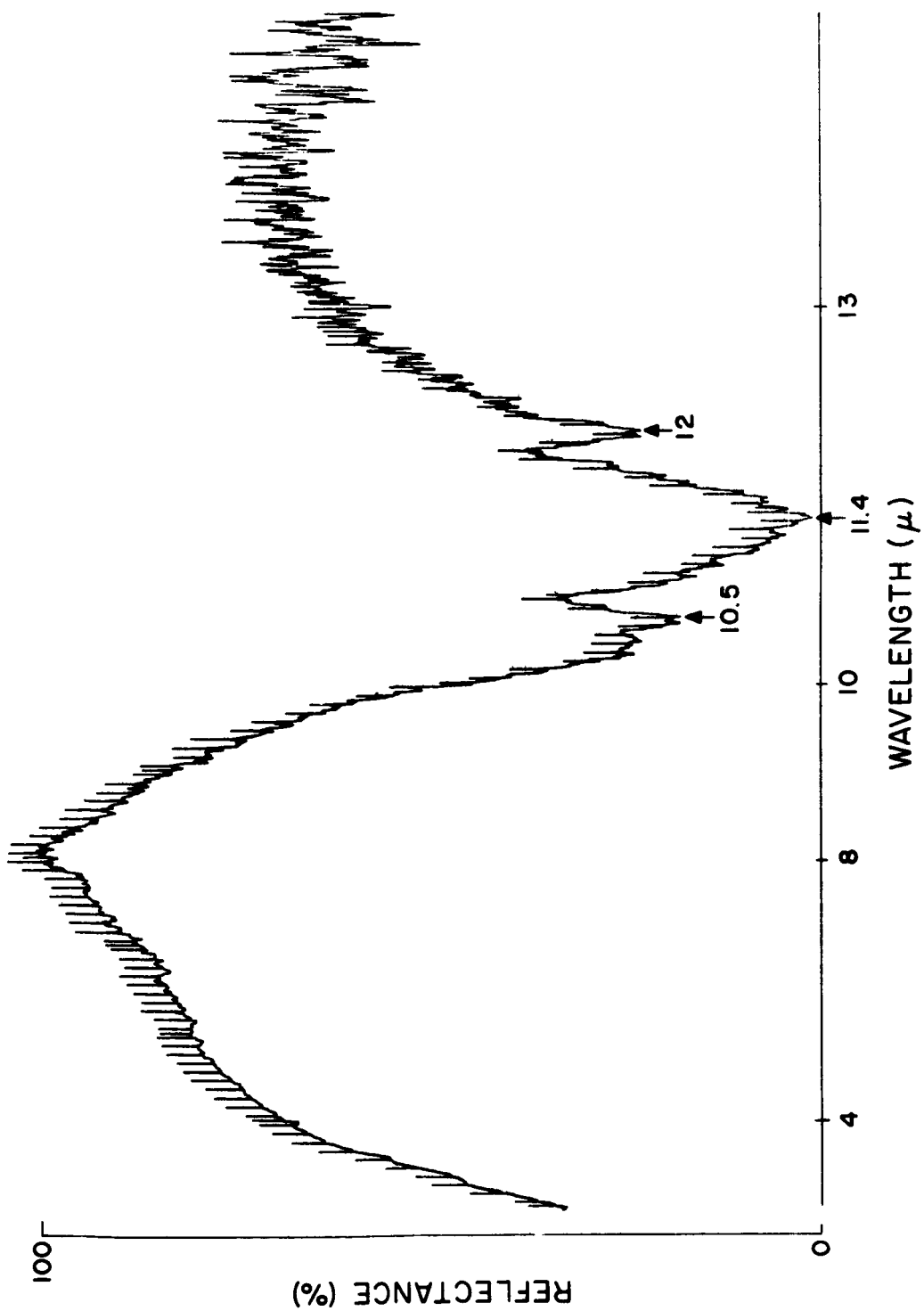


Figure 27: Internal Reflection Spectrum of Powdered Fayalite Using  $\theta = 45^\circ$  and KRS-5 Plate.

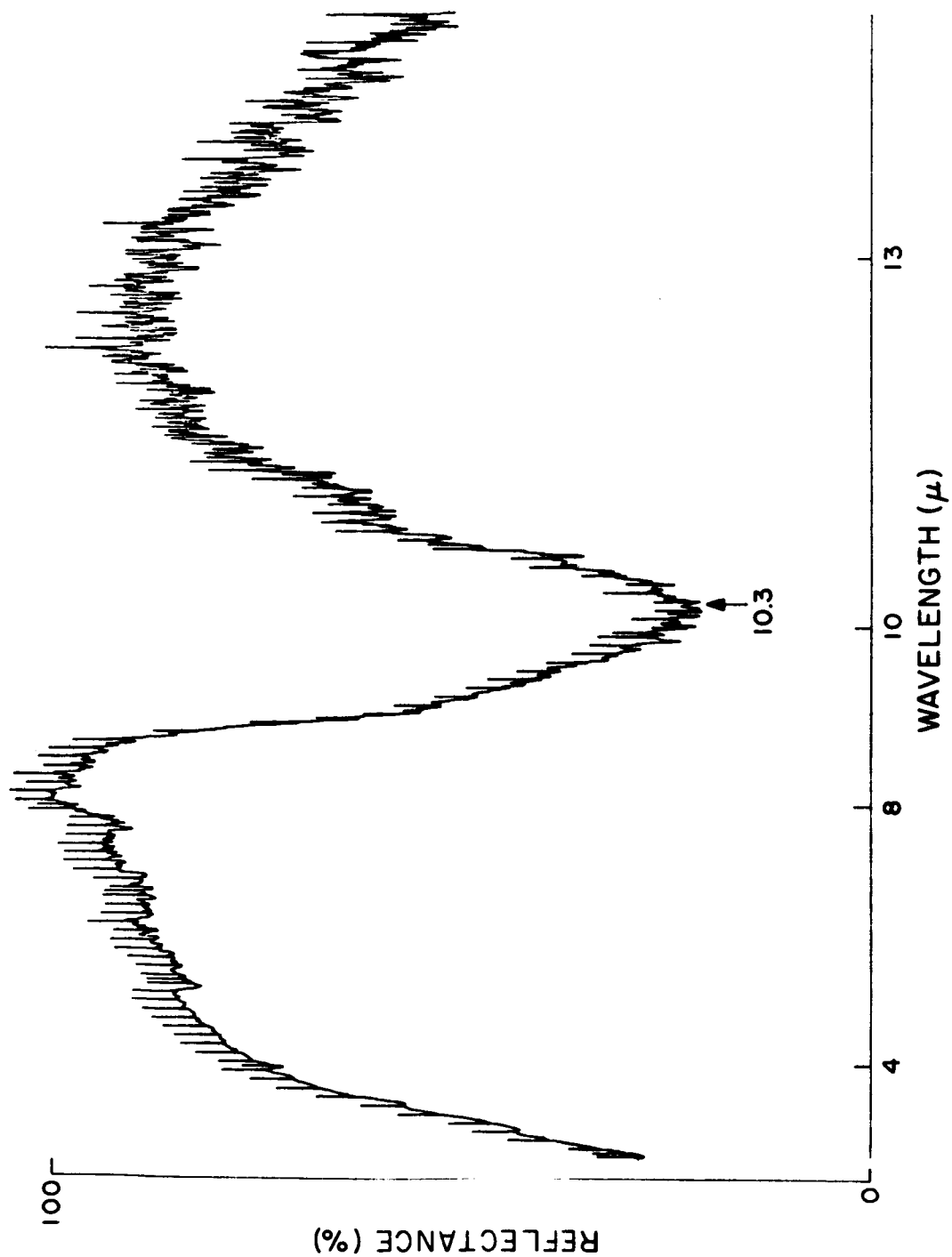


Figure 28: Internal Reflection Spectrum of Powdered Peridotite (PCC-1) Using  $\theta = 45^\circ$  and KRS-5 Plate

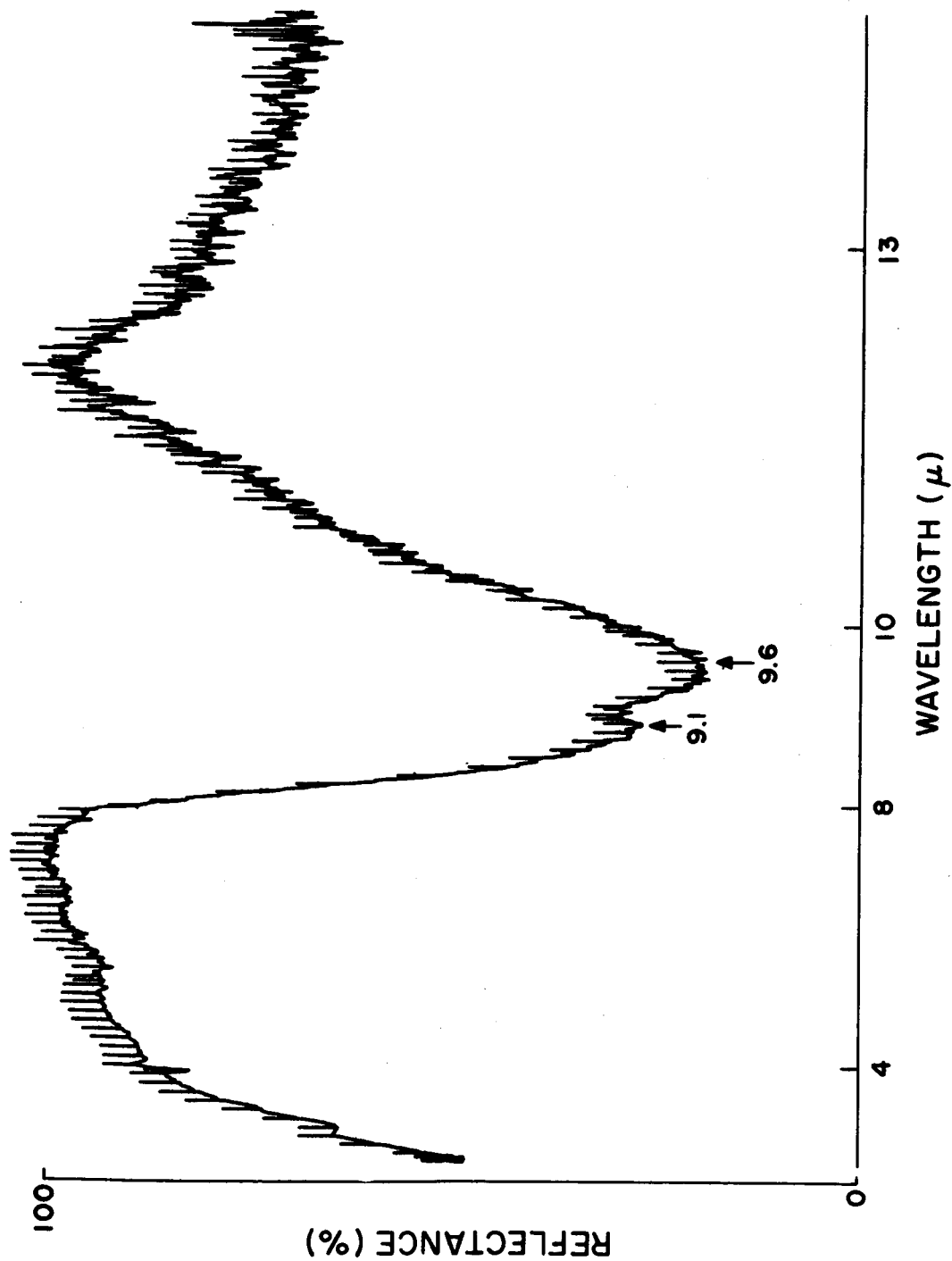


Figure 29: Internal Reflection Spectrum of Powdered Basalt (BCR-1) Using  $\theta = 45^\circ$  and KRS-5 Plate.

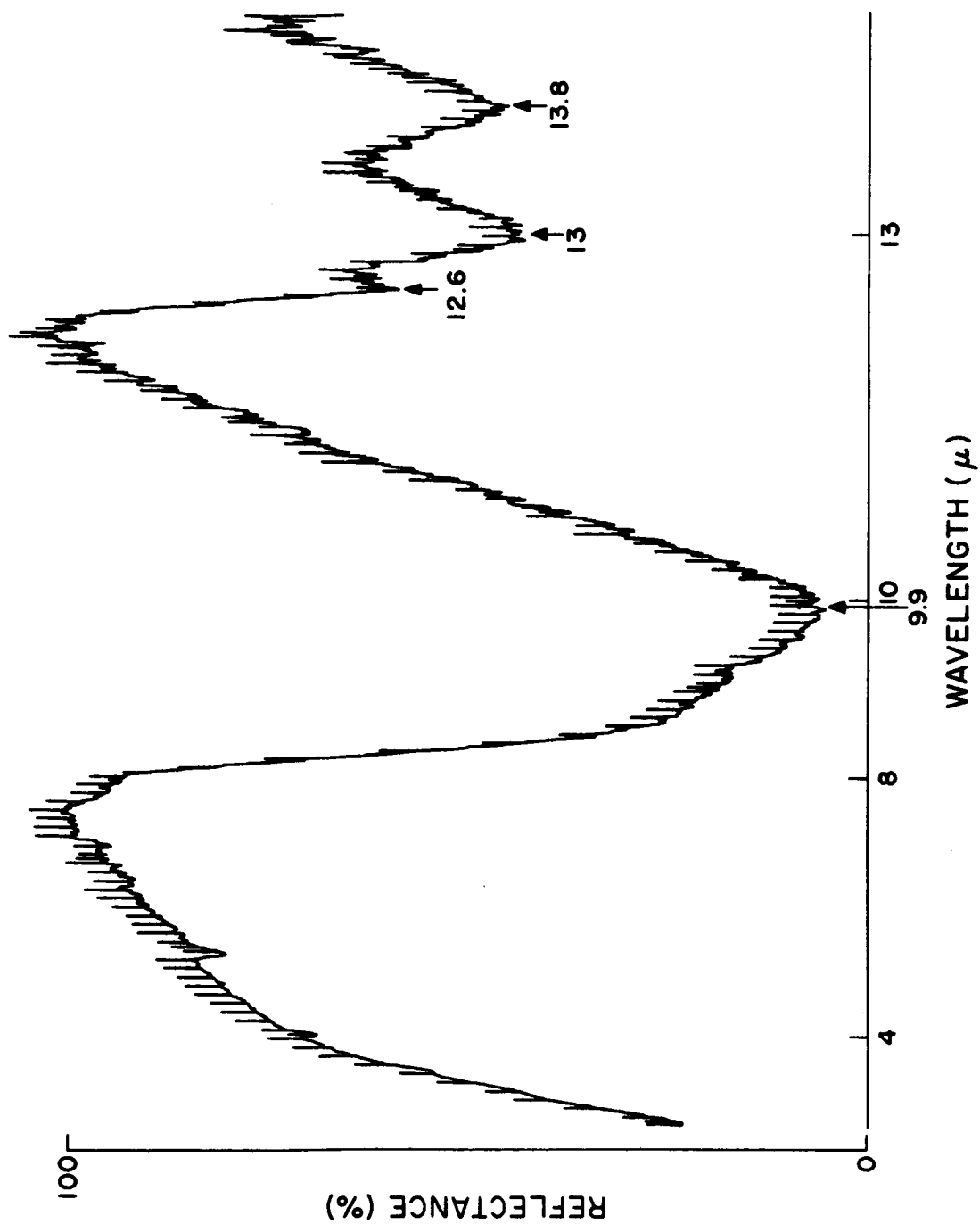


Figure 30: Internal Reflection Spectrum of Powdered Granodiorite (GSP-1) Using  $\theta = 45^\circ$  and KRS-5 Plate

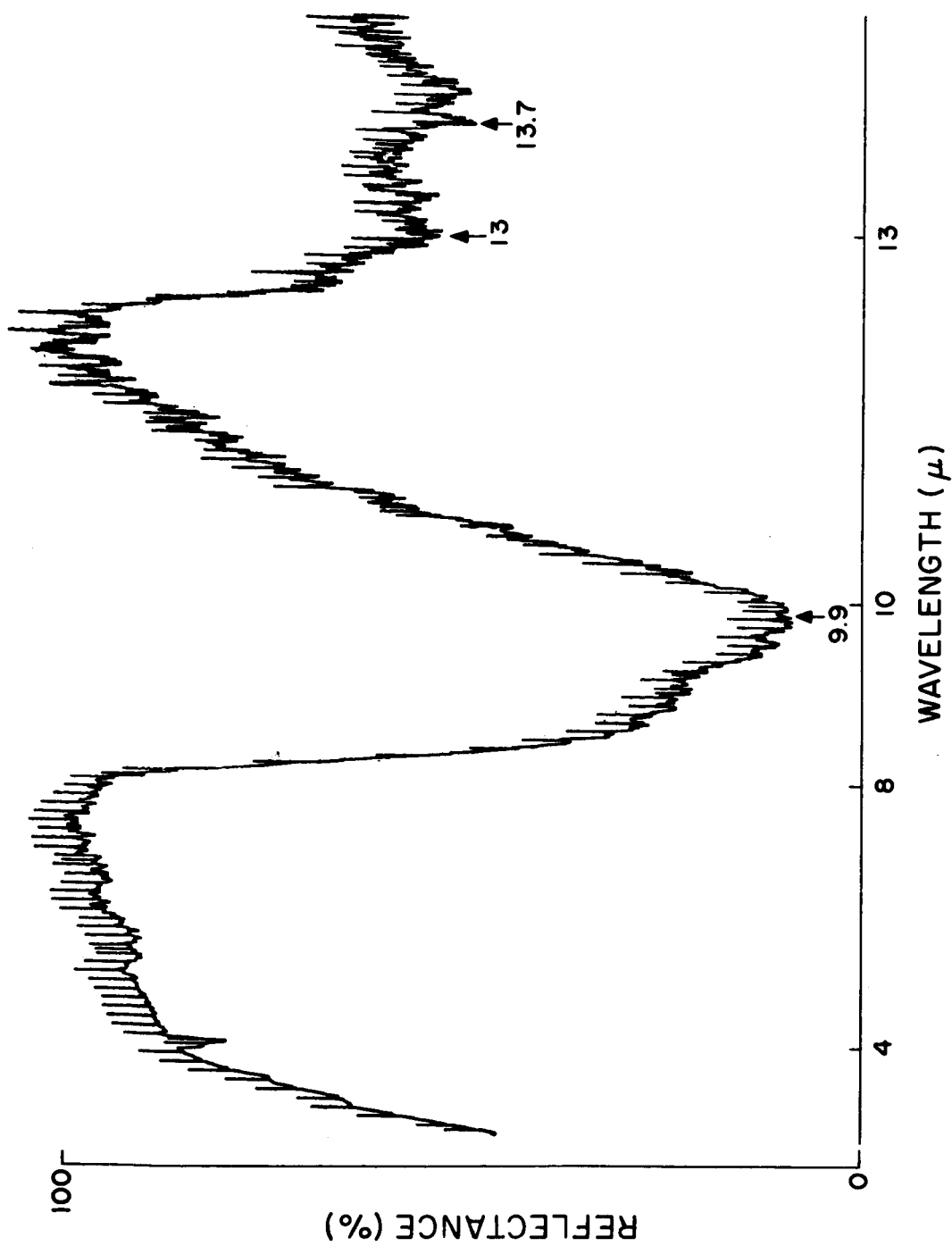


Figure 31: Internal Reflection Spectrum of Powdered Westerly Granite (G2)  
Using  $\theta = 45^\circ$  and KRS-5 Plate.

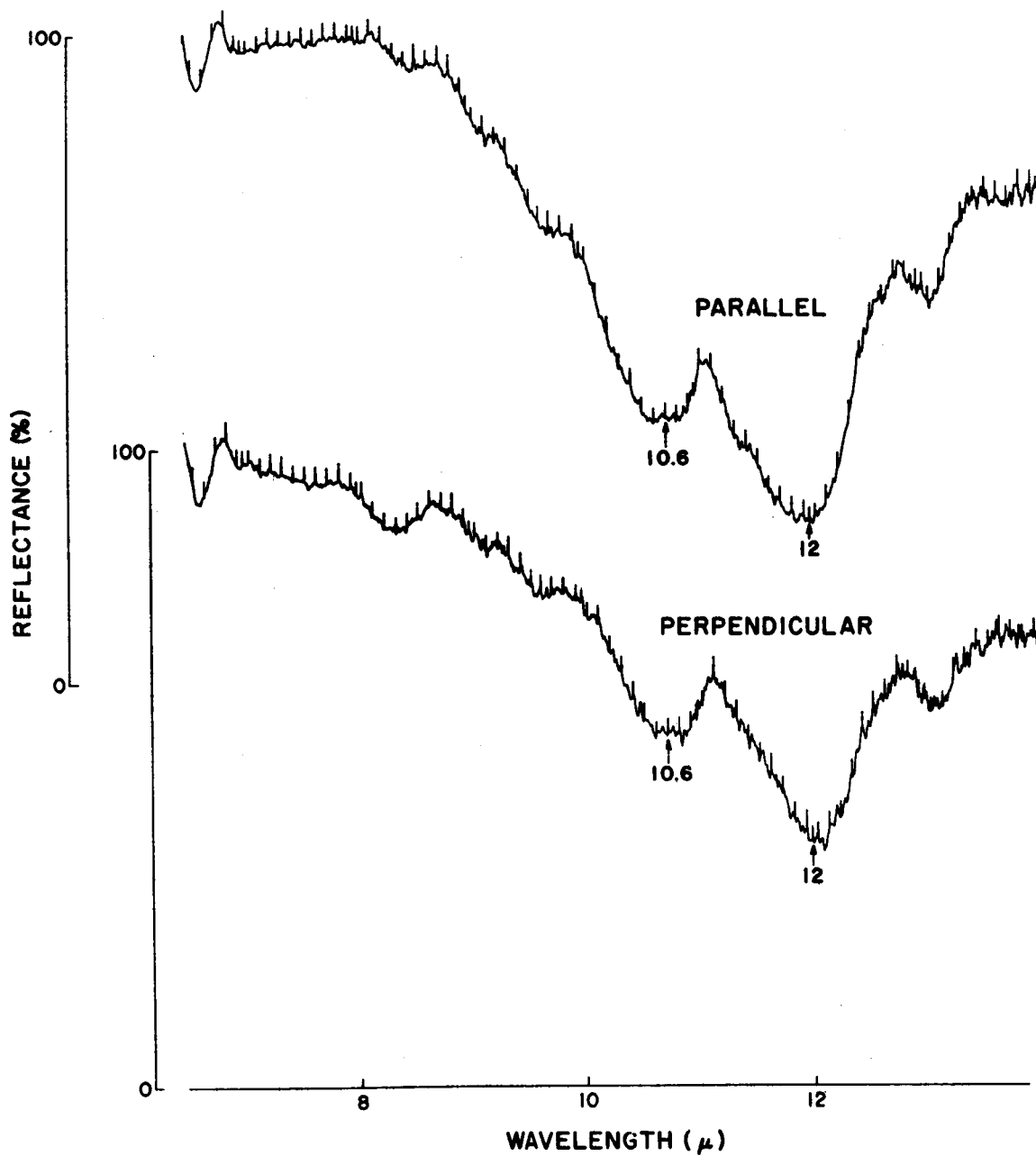


Figure 32: Internal Reflection Spectra of Powdered Fayalite Using  $\theta = 45^\circ$ , KRS-5 Plate and Perpendicular and Parallel Polarization.

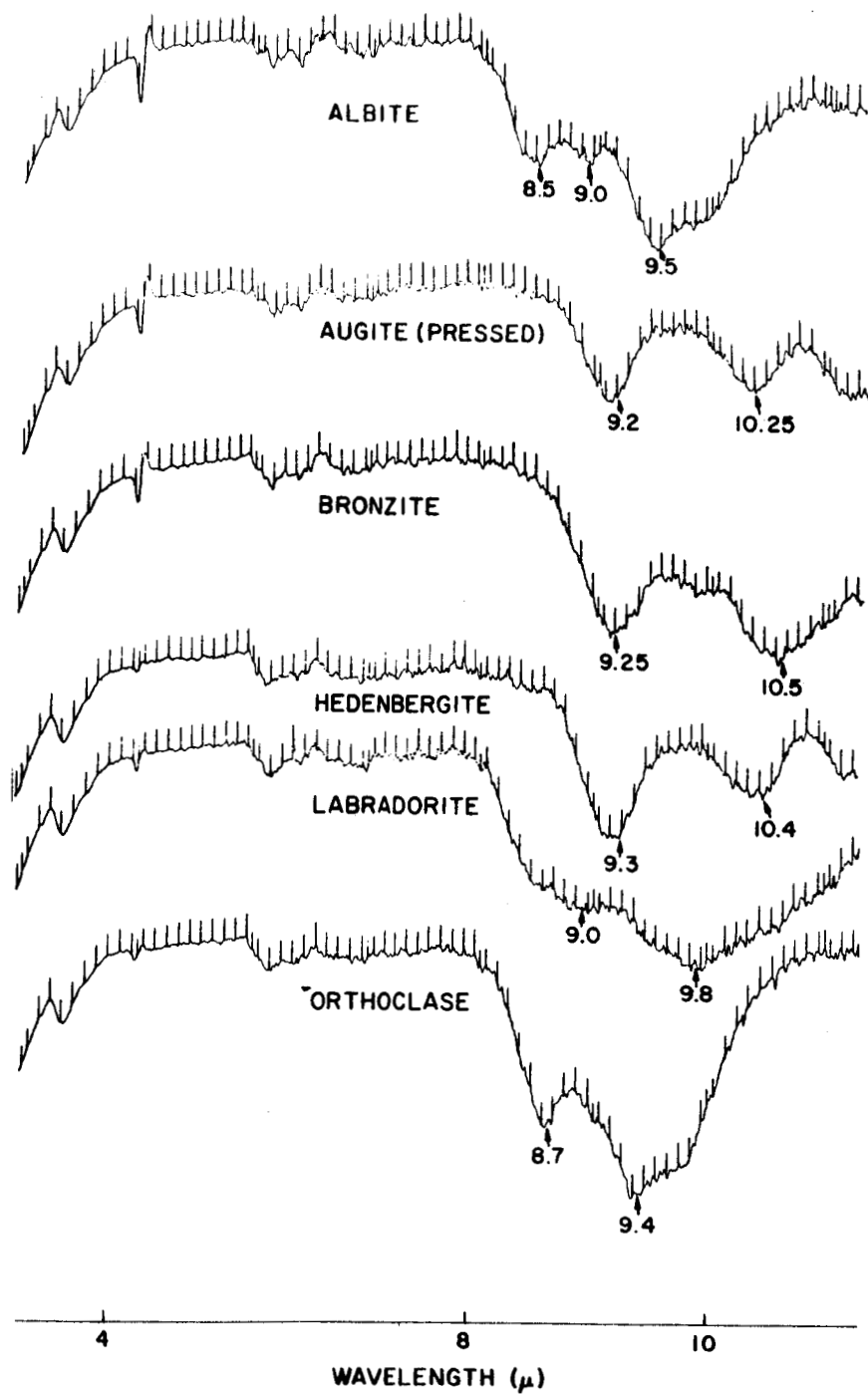


Figure 33: Internal Reflection Spectra of Powdered Rocks Using  $\theta = 45^\circ$ , Ge Plate and Parallel Polarization.



4. CONCLUSIONS

(1) The most important observation of this work is that there are little or no scattering losses in the non-absorbing regions by particulate on the surface of the internal reflection element, regardless of particle size. (The particle sizes studied included six fractions in the 0-43 $\mu$  range of the earlier work (NASW 964), and three fractions in the 0-30 $\mu$  range in the present work, as well as a number of unelutriated samples having particle sizes as large as 100 $\mu$  in diameter.) This observation verifies the conclusion of the previous work at  $\theta = 45^\circ$ . In the present work, measurements were extended to other angles-of-incidence and to polarized light.

Another important observation is that, in the absorbing regions, optical spectra could be recorded via internal reflection, regardless of particle size.

It is concluded that Internal Reflection Spectroscopy can be used to record spectra of particulate matter (e.g., rocks and minerals), and no sample preparation is required.

The importance of these findings can be further appreciated when it is realized that transmission spectra can be recorded only for very fine powders, and even these powders should preferably be embedded in some matrix (e.g., KBr, KRS-5, etc.) to minimize scattering losses. The lack of, or small degree of, scattering with the internal reflection measurements is further evidenced in other measurements where the spectra of porous, uneven paper, fibers and fabrics were obtained with no sample preparation.

(2) Although considerable time was spent in attempting to obtain a theoretical understanding of the little or no scattering losses for the internal reflection measurements, we were unable to obtain a theoretical explanation for this phenomenon. Scattering theory is, in general, very complicated; even for the simplest of models. A model and approach have been suggested in this report.

(3) Pertaining to the quartz spectra of this study, it can be said that these powders are pure quartz. This was verified and substantiated by our x-ray analysis and by transmission measurements using KBr pellets. Quartz was initially chosen because it has been extensively studied in the past. It was perhaps an unfortunate choice principally because there are such wide excursions

in the optical constants. This made it impossible to choose an internal reflection element material and angle-of-incidence for which the critical angle would remain below the angle-of-incidence, through the absorption bands.

One advantage in applying the internal reflection technique to the study of quartz powders is that spectra, although different, can be recorded for any particle size; this is not the case in transmission measurements where only fine powders can be used. In other materials containing silica, the vibrations should be more highly damped and large excursions in the refractive index will probably not occur. For example, measurements of Fayalite using polarized light showed, unlike quartz, similar spectra for both polarizations.

(4) The 90° out-of-phase chopper and detection system proved to be consistently stable to  $\pm 0.5\%$ . This system simplified the design of the laboratory spectrometer, and enabled us to obtain reflectance spectra in a simplified and direct manner.

(5) The ability to record spectra of the fourteen (14) minerals and rocks provided by NASA - where no attempt was made to fractionate the powder - provided a practical demonstration of the usefulness of Internal Reflection Spectroscopy for examining powdered minerals and rocks.

5. RECOMMENDATIONS

A continuation of these studies should include the following proposed recommendations:

- a) Select a powdered material whose optical constants do not have such large excursions as those of quartz. Elutriate the powder and conduct studies similar to those made with the kaolinite-quartz mixtures and quartz. Possible materials for this purpose might be calcite, silicon carbide or sapphire.
- b) Conduct a carefully controlled experiment in an attempt to place an upper limit on the degree of scattering, if any, stemming from the interaction of the evanescent wave with the particulate matter on the surface of the internal reflection element. This might be done, for example, by depositing the particulate matter on the surface of the element with the aid of an electrostatic precipitator (Ref. 15).
- c) Regarding measurements of optical constants, it would seem advisable to first measure the optical constants of a solid isotropic mineral via internal reflection and to then examine the mineral in powdered form. One reason for this procedure is that the nature of the contact between two solid materials can be controlled and determined more easily than the contact between powder and solid material.
- d) One area that has not yet been investigated for scattering, via internal reflection, is that of very fine powders - this should be studied.
- e) To improve the sensitivity of the instrumentation, we propose the use of a mercury-doped germanium detector cooled via a Cryogem - a Stirling cycle cryogenic cooler developed at Philips Laboratories (Ref. 16).
- f) The possibility of using Internal Reflection Spectroscopy for detection of water and organic material in the lunar soil was discussed at the NASA 1965 Summer Conference on Lunar Exploration and Science (Ref. 17). A determination of the sensitivity required for this purpose should be made, and experiments should be conducted to check the feasibility of this approach.

6. REFERENCES

1. Philips Laboratories, Division of North American Philips Co., Inc., "Final Report for Study Program to Obtain the Infrared Absorption Spectra of Powdered Rocks", N.J. Harrick, TR174, NASA contract NASW-964, Briarcliff Manor, N.Y., Dec. 1964.
2. N.J. Harrick and N.H. Riederman, "Infrared Spectra of Powders by Means of Internal Reflection Spectroscopy", Spectrochim. Acta 21, 2135 (1965).
3. N.J. Harrick, "Variable Angle Attachment for Internal Reflection Spectroscopy", Analytical Chemistry 37, 1445 (1965).
4. M. Born and E. Wolf, "Principles of Optics", The MacMillan Co., New York, 1964, 2nd ed.
5. N.J. Harrick, "Electric Field Strengths at Totally Reflecting Interfaces", J. Opt. Soc. Am. 55, 851 (1965).
6. W.N. Hansen, "On the Determination of Optical Constants by a Two-Angle Internal Reflection Method", Spectrochim. Acta 21, 209 (1965).
7. J. Fahrenfort and W.M. Visser, "On the Determination of Optical Constants in the Infrared by Attenuated Total Reflectance", Spectrochim. Acta 18, 1103 (1962).
8. W.N. Hansen, "Internal Reflection Spectroscopy and the Determination of Optical Constants", ISA TRANS. 4, 263 (1965).
9. I. Simon and H.O. McMahon, "Study of the Structure of Quartz, Cristobalite, and Vitreous Silica by Reflection in Infrared", J. Chem. Phys. 21, 23-30 (1953).
10. I. Simon, "Spectroscopy in Infrared by Reflection and Its Use for Highly Absorbing Substances", J. Opt. Soc. 41, 336-345 (1951).

PHILIPS LABORATORIES

11. W.G. Spitzer and D.A. Kleinman, "Infrared Lattice Bands of Quartz", Physical Review 121, 1324-35 (1961).
12. H. Nassenstein, "Verfahren zur Bestimmung der optischen Konstanten von feinverteilten absorbierenden Feststoffen", Naturwissenschaften 52, 511 (1965).
13. J.M. Hunt, M.P. Wisher, and L.C. Bonham, "Infrared Absorption Spectra of Minerals and Other Inorganic Compounds", Analytical Chemistry 22, 1478-97 (1950).
14. P.J. Launer, "Regularities in the Infrared Absorption Spectra of Silicate Minerals", The American Mineralogist 37, 764-84 (1952).
15. Philips Laboratories, Division of North American Philips Co., Inc., "Final Report for Research on Detection of Trace Quantities of Toxic Materials", N.J. Harrick, TR177, Melpar Contract SU-603907/63, Briarcliff Manor, N.Y., Aug. 1964.
16. F.K. du Pré and A. Daniels, "Miniature Refrigerator Opens New Possibilities for Cryo-Electronics", Signal Mag., 20, 10 (1965).
17. National Aeronautics and Space Administration, "NASA 1965 Summer Conference on Lunar Exploration and Science", NASA Report SP-88, p. 272, Falmouth, Mass., July 19-31, 1965.